NASA Contractor Report 198265

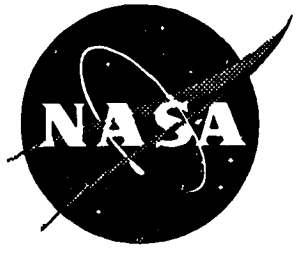

Evaluation of the Impact Response of Textile Composites

M. A. Portanova
Lockheed Martin Engineering and Sciences Company, Hampton, Virginia

Contract NAS1-19000

December 1995

National Aeronautics and
Space Administration
Langley Research Center
Hampton, Virginia 23681-0001

Introduction

Holes, notches, or impact induced damage can severely degrade the structural integrity of conventional laminated graphite fiber reinforced epoxy composites. Because of this, relatively low design strains are imposed. To obtain the weight saving benefits associated with graphite/epoxy materials there is a need to improve the damage tolerance and delamination resistance of these materials. Attempts to accomplish this through the introduction of toughened epoxy resins has been very expensive. Another approach has been to incorporate through-the-thickness reinforcement such as in textile composites.

This paper will address the impact damage resistance and damage tolerance of three different textile composite material forms. The material forms tested were stitched and unstitched uniweaves, 2-D braids, and 3-D weaves. Four different thicknesses of the uniweave material were tested. With the braids and weaves, only one thickness was evaluated but several variations of braiding and weaving parameters were tested. All the materials were subjected to either quasi-static indentation or low velocity (large mass) impacts and then loaded in tension or compression to measure their residual strengths.

The uniweave composites were made from dry carbon fabric. The carbon tows were held in place with a fill direction yarn, braided normal to the tows. The 2-D and 3-D fabrics were made by braiding or weaving carbon tows. The braids were made by braiding layer over layer to achieve the desired thickness. The weaves were woven to the desired thickness in a single pass. Three different through-the-thickness weave types were evaluated. These were an angle interlock, orthogonal interlock, and layer to layer interlock. All the composites were made using a resin transfer molding process.

All specimens were impacted or indented using an instrumented tup containing a 0.5 inch diameter hemispherical tip. The low velocity impacts were done with a instrumented falling weight, dropped from a predetermined height. The static indentations were performed in a servo hydraulic load frame under stroke control. All specimens were clamped firmly in an aluminum picture frame test fixture for impacting. Damage resistance was determined through the application of ultrasonic through transmission C-scans. Damage tolerance was determined by measuring the materials ability to support load for a given damage state.

Description of Materials

2-Dimensional Triaxial Braids

All of the 2-D fabric preforms were braided by Fiber Innovations Inc., Norwood, MA. The test panels were resin transfer molded (RTM) using Shell RSL-1895 epoxy resin and cured at Boeing Defense and Space Group in Seattle, WA. Details of Boeing's manufacturing process can be obtained from Ref. [1], "Resin Transfer Molding of Textile Composites". An illustration of a typical 2-D braid is given in Figure 1.

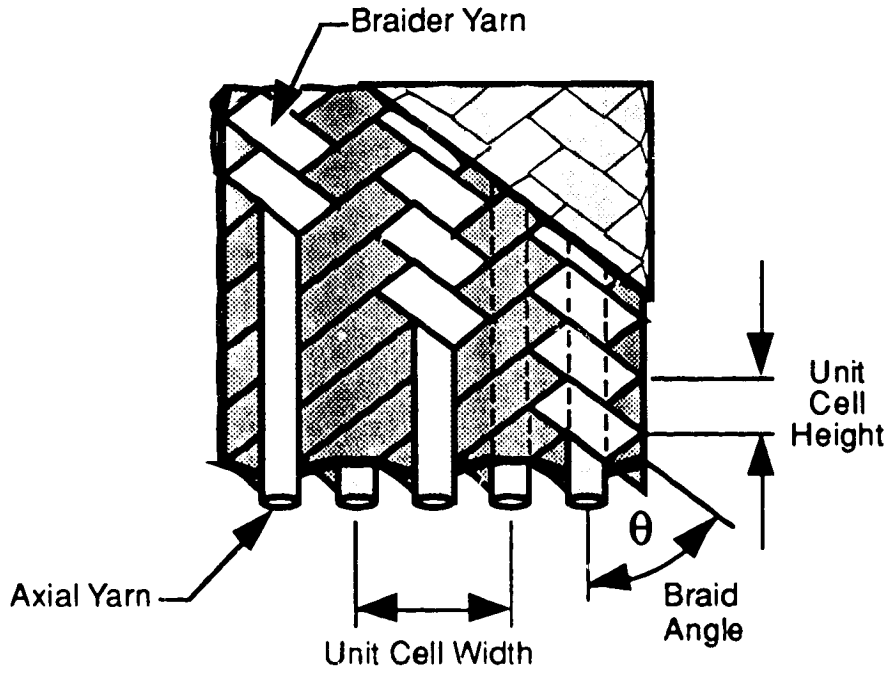

Figure 1. Illustration of a Typical 2-D Triaxial Braid Configuration.

In Table 1, the following nomenclature has been adopted to describe the layup:

$$[0_{XXK}/\pm\theta_{XXK}]\ Y\%\ \text{Axial}$$

Where XX indicates the yarn size, K indicates thousands and Y indicates the percentage of axial yarns in the preform.

The three letters preceding the "[$0_{XXK}/\pm\theta_{XXK}$] Y% Axial" nomenclature in Table 1 are intended as abbreviations where "S" and "L" mean "Small" and "Large", respectively. For example, the SLL [$0_{30K}/\pm70_{6K}$]46% braid is deciphered as containing a small (6K) braider yarn, a large (46%) percentage of axial yarns, and a large (70°) braid angle.

Four different braided architectures were evaluated but at only one laminate thickness. The desired plate thickness was achieved by stacking layers of braided fabric to obtain a nominal 0.25 inch thickness after curing. The specifics of each of the braiding parameters are given in Table 1. Axial tow size and content, expressed as the percentage of total yarn content, as well as braided tow size were varied in an attempt to evaluate the effect of yarn size. The intent was to make comparisons between two or more braids based on a single variation in their construction. For example, the SLL and LLL both have 46% axial and a 70° braid angle but the LLL is constructed using tows that are 2.5 times as large as those in the SLL material. This difference should allow an investigation of the effect of tow size on impact performance. Differences in architecture exist between the other braids as well.

Table 1. Boeing's 2-D Braided Composites Architectures.

Braid Code	Axial Tow Size	Braided Tow Size	% Axial Tow	Braid Angle [°]	Unit Cell Width [in]	Unit Cell Length [in]
SLL [$0_{30K}/\pm70_{6K}$]46%	30 K	6 K	46	0±70	0.458	0.083
LLS [$0_{36K}/\pm45_{15K}$]46%	36 K	15 K	46	0±45	0.415	0.207
LLL [$0_{75K}/\pm70_{15K}$]46%	75 K	15 K	46	0±70	0.829	0.151
LSS [$0_{6K}/\pm45_{15K}$]12%	6 K	15 K	12	0±45	0.415	0.207

3-Dimensional Interlocking Weaves

Three different 3-D woven composites were evaluated in this investigation. As with the braids, only one thickness was tested. Each 3-D architecture was woven to its desired thickness in a single pass, thus the weaves did not contain interfaces between plies. All three architectures provide true through-the-thickness reinforcement by interlacing yarns in the z direction. An illustration of each of the different configurations is shown in Figure 2. Tow size

and content, expressed as the percentage of total yarn content, along with an architectural description of each are provided in Table 2. The preforms were produced by Textiles Technologies Inc. and, like the 2-D braids, they were resin transfer molded at Boeing using Shell RSL-1895 epoxy and cured.

Note that in an attempt to measure yarn size effects, the weaves were constructed in pairs with the "-1" materials having yarn bundles twice as large as the "-2" materials. This allowed an evaluation of not only the different woven architectures but the effect of tow size as well. The different architectures were designed with a constant tow size in each of the warp, weft, and weaver tows while the proportion of fibers was slightly varied when needed to maintain balance in the architectures. This consistency in constituents allows a comparison between each of the 3-D architectures.

Table 2. Description of the 3-D Interlock Woven Materials.

Name	Description	Warp Tow	Weft Tow	Weaver Tow
OS-1	Through-the-thickness orthogonal interlock	24 K (59%)	12 K (33%)	6 K (7.4%)
OS-2		12 K (58%)	6 K (37%)	3 K (6.1%)
TS-1	Through-the-thickness angle interlock	24 K (57%)	12 K (33%)	6 K (9.8%)
TS-2		12 K (56%)	6 K (38%)	3 K (5.8%)
LS-1	Layer-to-layer interlock	24 K (58%)	12 K (34%)	6 K (6.8%)
LS-2		12 K (57%)	6 K (36%)	3 K (5.9%)

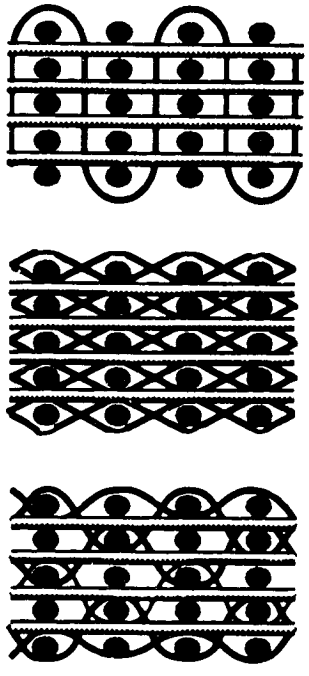

Figure 2. Illustration of the 3-D Interlocking Woven Materials.

Stitched Uniweaves

The uniweave fabric was produced by Textile Technologies Inc. and then resin transfer molded at Boeing. The materials tested were constructed from AS4/3501-6 graphite epoxy. The uniweave fabric consisted of plies of unidirectional graphite fibers, held together with a light fiberglass yarn woven in the fill direction. Several layers of fabric were stacked to create quasi-isotropic $[+45/0/-45/90]_{xs}$ lay-ups. Four thicknesses were evaluated; where x = 6, 4, 3, and 2. Each thickness was tested in both stitched and unstitched forms.

The average specimen thicknesses for each of the stitched and unstitched materials are given below in Table 3. Stitching of the uniweaves was performed by Cooper Composites in Seattle, WA. The specifics of the stitched preform are described below in Table 4. An illustration of a typical stitched uniweave is shown in Figure 3.

Table 3. Average Thickness of Stitched and Unstitched Uniweaves.

Ply Count	Stitched	Unstitched
[+45/0/-45/90]6s	0.295 in.	0.267 in.
[+45/0/-45/90]4s	0.202 in.	0.180 in.
[+45/0/-45/90]3s	0.156 in.	0.135 in.
[+45/0/-45/90]2s	0.104 in.	0.092 in.

Table 4. Description of the Stitched Uniweaves.

Name	Stitch Material	Pitch Spacing Stitches per inch	Stitch Spacing [in]	Stitch Tow Size
SU-1	S2 Glass	8	0.125	3 K

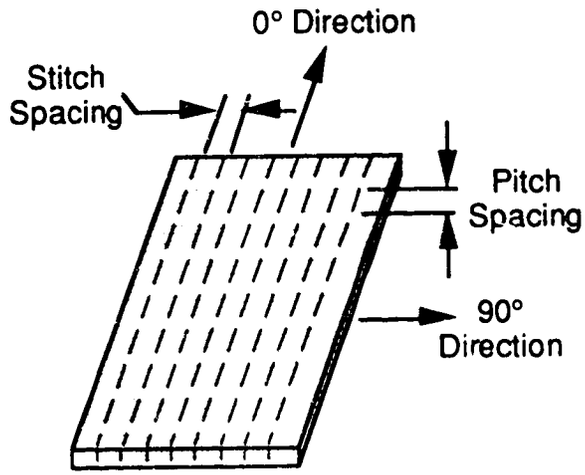

Figure 3. Illustration of the Stitched Uniweave Impact Specimen.

Test Specimen Configuration & Testing Methodology

Impact Testing

Both static indentation and falling weight impact tests were performed for this investigation. An illustration of the static indentation and compression after impact specimens are given in Figure 4. The static indentation specimen was slightly shorter than the falling weight impact specimen. The tension after impact specimen (not shown) was 9.0 inches long in the 0° direction, to allow for griping in the load frame. Both testing methods used the same instrumented tup and 1/2 inch diameter indenter. During testing each specimen was clamped in an aluminum test frame. The specific of each test method are given in the following sections.

In general, the method employed in this program was to perform repeated static indentation tests to obtain various amounts of damage. This damage was then documented and impact energies were determined for falling weight impacting. After falling weight impacting, each specimen was loaded to failure in either tension or compression to determine the damage tolerance of the material.

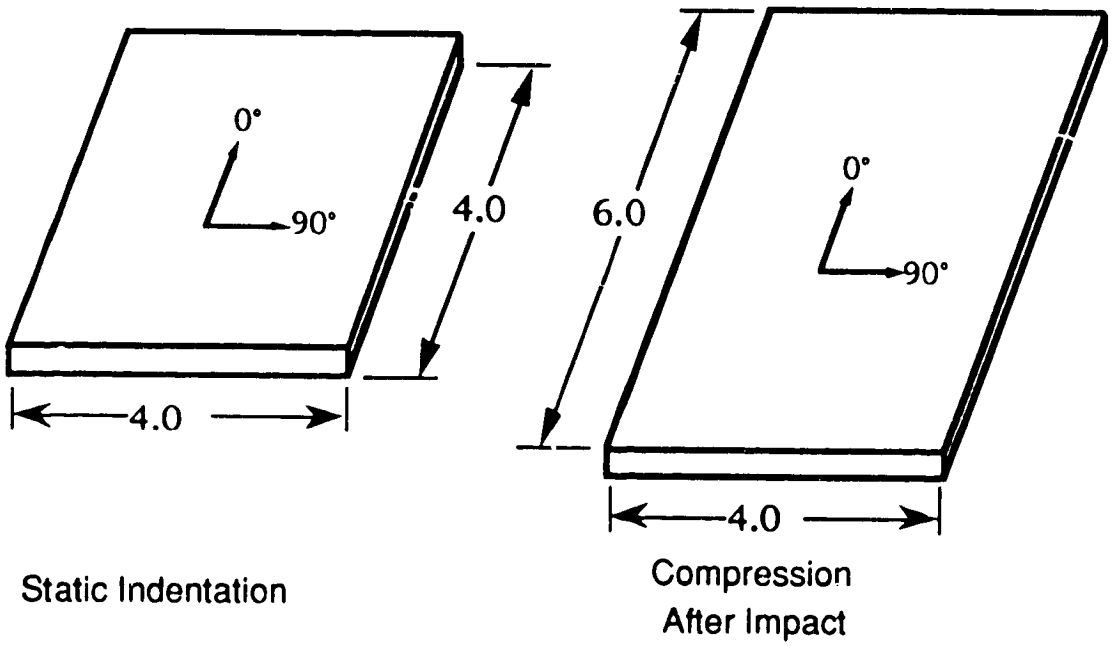

Figure 4. Illustration of the Static Indentation and Compression After Impact Test Specimen.

Static Indentation Tests

The test fixture used for the static-indentation portion of this test program is shown in Figure 5. This fixture contained a 3 x 3 in. opening with corner radius of 0.5 inch. The 4 x 4 in. panels, illustrated in Figure 4, were mounted in the test fixture and the bolts were torque tight to approximately 80 in•lbs. The instrumented impactor was centered in the top grip of a servo-hydraulic load frame, directly above the test specimen. The lower grip held a platen, supporting the clamped test specimen. The lower grip was ramped upward at 0.02 in/min. into the instrumented impactor. The instrumented impactor, or tup, as shown in Figure 5, was capable of measuring the impact force. This impact force was recorded using a digital data storage oscilloscope. The data was then reduced on a desk top computer using commercial software.

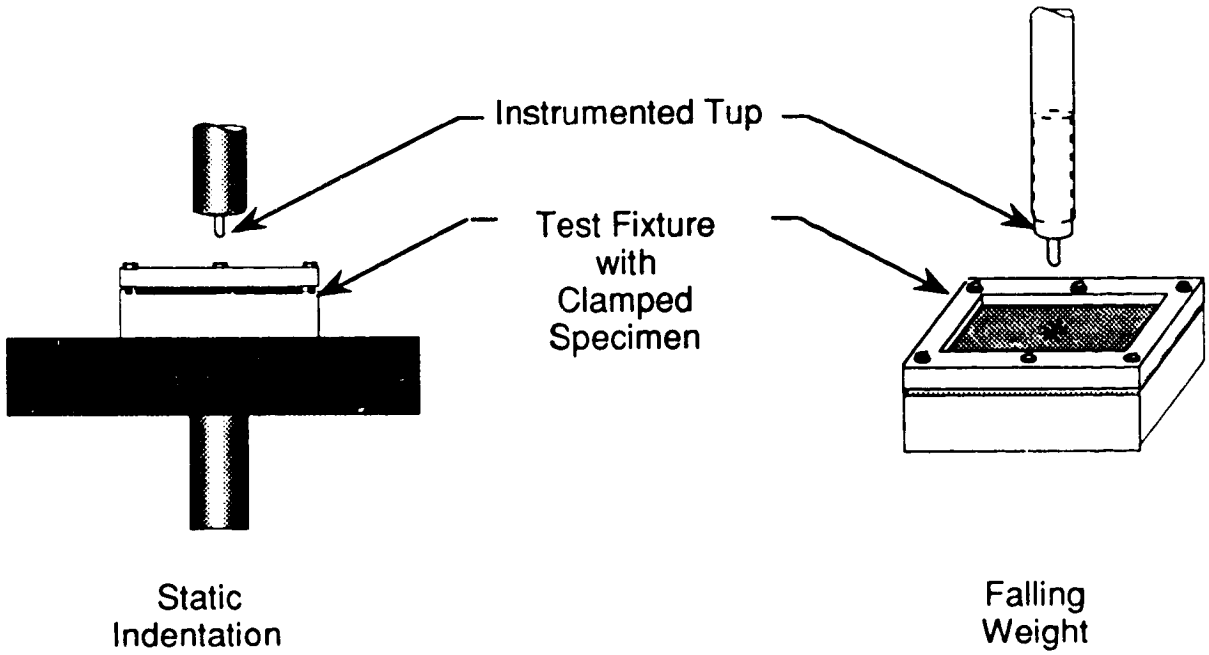

Figure 5. Illustration of the Static Indentation and Falling Weight Test Fixtures.

Falling Weight Impact Tests

The test fixture used for the falling weight impact portion of this study contained a 5 inch by 3 inch opening with each corner radius of 0.5 inch. A free falling mass impacted the specimen. An illustration of the impactor set-up and test fixture is given in Figure 5. The impactor consisted of three basic parts: a 2 inch diameter steel rod, an instrumented section, and a 1/2 inch diameter spherical tip. The impactor had a total mass of 11.67 lbm. The instrumented section, or tup, as shown in Figure 5, was capable of measuring the impact force. This impact force was recorded using a digital data storage scope. The data was then reduced on a desk top computer using commercial software.

The 4 x 6 inch panels were mounted in the holder illustrated in Figure 4 and the bolts were torque tight to approximately 80 in•lbs. The instrumented impactor was centered above the panel at the required height to impart the desired impact energy. After the impactor struck the specimen, a dummy panel was quickly moved between the fixture and specimen to prevent the impactor from repeatedly hitting the panel.

Impact Energy Calculations

The data taken from the static indentation tests were used to determine the falling weight energies required to produce pre-determined dent depths in the textile materials. In most cases multiple loading cycles were performed on a specimen until the desired, pre-determined amount of damage was attained. C-scans were taken between each loading excursion to measure the damage area.

Figure 6 is a plot of indentation force versus displacement of the indenter for a typical static indentation test. This figure contains histories for two loadings. The first loading, indicated by the solid line, shows an initial load drop at approximately 5 kN. This is indicative of the onset of large damage growth. After this first load drop, load increases up to a point where the surface of the plate is no longer capable of supporting the indentation force. At this point damage typically grows in the form of delamination and matrix cracking and typically the surface is dented.

After the first loading cycle, the specimen was removed, C-scans and surface dent depth measurements were taken. The same specimen was then reloaded to further grow the damage or dent depth to some pre-determined level. The loading history of the second load excursion is shown in Figure 6 as a dashed line. Arrows have been added to show the loading direction. The load increases up to the point that the prior loading left off. Once this load is reached damage accumulation continues and the depth of the surface dent is increased. At this point, the specimen is once again unloaded and measurements are retaken to determine if further loading is required. In some cases three or four load excursions were required to reach the desired dent depth of 0.10 inch.

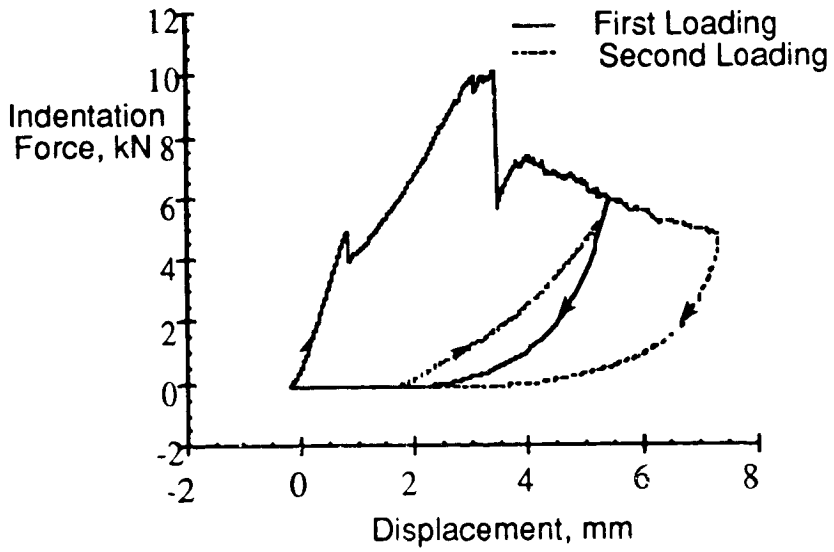

Figure 6. Load-Displacement History Of A Static Indentation Test.

Figure 7 features the combined results of the two loading excursions shown in Figure 6. The work done is given by the expression:

$$\text{Total work} = \int_0^x P dx \qquad (1)$$

where P is the applied load and x is the displacement of the plate in the loading direction.

Neglecting viscoelastic effects and the inertia of the plate, the work in Equation (1) is equal to the kinetic energy of the impactor at contact. The area under the curve in Figure 7 was integrated using Equation (1) to estimate the equivalent kinetic energy for the falling weight impacts to obtain pre-determined dent depths for Barely Visible Impact Damage (BVID) and Visible Impact Damage (VID) impacts. The energy needed to obtain these average dent depths are given in Tables 4 and 5. It is important to notice in Table 4 that because thickness decreases with ply count, the impact energy required to produce a given surface dent or damage area also decreases. Comparisons are made here in terms of dent depth and not impact energy.

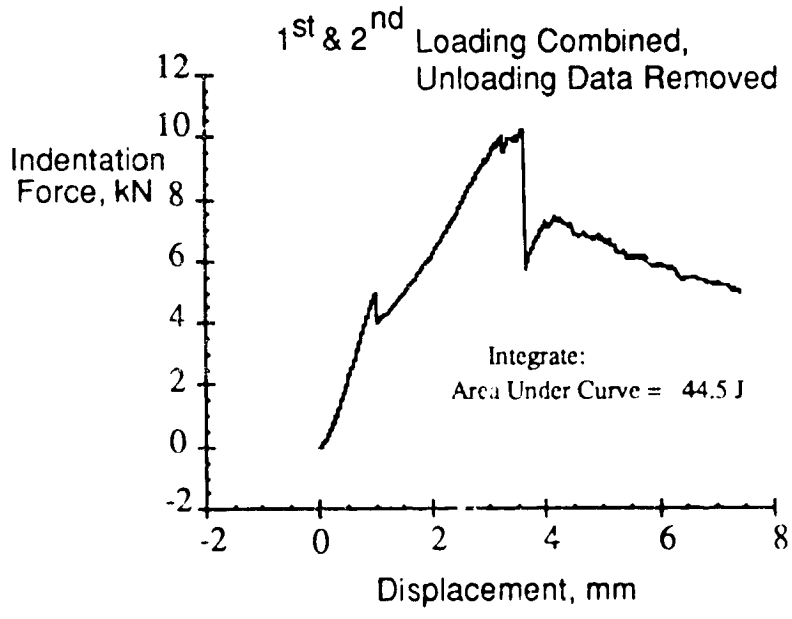

Figure 7. Load-Displacement History Of A Static Indentation Test With First And Second Load Excursions Combined.

Figure 8 is a plot of impact force vs. time for a 48 ply stitched uniweave impact at 15.39 ft•lbf. The response shown is typical of a stitched uniweave. The force-deflection curve for this experiment should be similar to that shown in Figure 7. The amount of peak force obtained is a function of the extent of damage to the test coupon from the impact event. Thus, a more damage resistant material will have a higher peak impact force when impactor parameters and undamaged plate stiffness are equal.

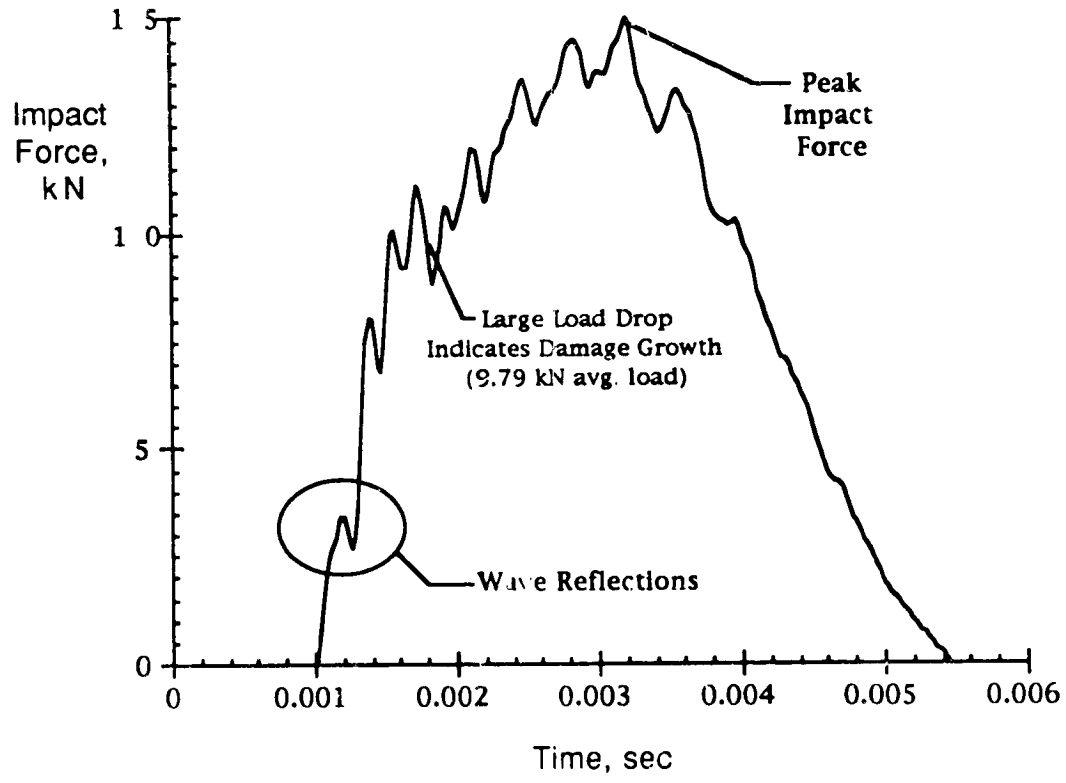

Figure 8. A Plot Of Falling Weight Impact Force Versus Time For A 48 Ply Stitched Uniweave Impacted At 15.39 Ft•Lbf.

Two impact energies were determine from the static indentation tests. The first produced on average a 0.10 inch deep dent in the specimen. The second produced a barely measurable surface dent. These shallow dents were only a few thousandths of an inch deep. A few specimens were also impact at an intermediate or Mean energy.

For the purpose of this paper, the term Visible Impact Damage or VID refers to an impact energy sufficient to produce an average dent depth of 0.10 inch. The term Barely Visible Impact Damage or BVID refers to an impact energy sufficient to produce damage barely measurable by C-Scan. The Mean Impact Energies are mean values based on the average of the VID and BVID energies. The average dent depths and each of the impact energies used on each of the various materials are given in Tables 4 and 5 below.

Table 4. Falling Weight Impact Energies For Uniweaves.

Material	BVID	Mean	VID
48 ply Stitched 48 ply Unstitched	15.39 ft•lbs	39.12 ft•lbs	62.86 ft•lbs
32 ply Stitched 32 ply Unstitched	7.29 ft•lbs	18.77 ft•lbs	30.26 ft•lbs
24 ply Stitched 24 ply Unstitched	5.48 ft•lbs	13.29 ft•lbs	21.11 ft•lbs
16 ply Stitched 16 ply Unstitched	3.00 ft•lbs	7.43 ft•lbs	11.87 ft•lbs

Note:

BVID : Barely Visible Impact Damage, Dent depths ≈ 0.005 in.
Mean : Mean Impact Damage, Dent depths ≈ 0.04 in.
VID : Visible Impact Damage, Dent depths ≈ 0.10 in.

The values used to impact the 2-D braids and 3-D weaves were chosen to allow a direct comparison with the results from the 48 ply uniweaves. Each was of similar thickness, thus, the differences between the impact responses should be an effect of the difference in material architectures.

Table 5. Falling Weight Impact Energies For Braids & Weaves.

Material	BVID	VID
2-D Braids	15.39 ft•lbs	62.86 ft•lbs
3-D Weaves	15.39 ft•lbs	62.86 ft•lbs

Note:

BVID : Barely Visible Impact Damage, Dent depths ≈ 0.009 in.
VID : Visible Impact Damage, Dent depths ≈ Penetration

Damage Assessment Method

Each panel was ultrasonically C-scanned before impact to ensure that the panels were of high quality, free from manufacturing defects that would lead to premature failure. C-scans after impact were used to determine the extent of the impact damage. Area calculations of the damage were made from the through-the-thickness ultrasonic projections. This method does not account for the total amount of damage in the specimen. It only shows a shadowing of the largest damaged areas. Although this is not an accurate account of the total damage, it is however accepted as an accurate and repeatable way of comparing the results for a given impact energy.

Compression and Tension After Impact Testing

After impacting, each of the falling weight impact test specimens were loaded to failure in a closed-loop servo-hydraulic testing machine run in stroke-control. All testing was conducted at room temperature, dry conditions. Load cell output and machine stroke were recorded using a digital data storage oscilloscope that allowed dynamic measurements during the test.

The compression specimens were mounted in a special test fixture to prevent global buckling of the test coupon during loading. This standard NASA compression after impact test fixture (Ref. 2) is illustrated in Figure 9. Because of the large length and width of the CAI coupons (as compared to their thickness) buckling was observed in the 16 ply uniweaves and some of the 24 ply uniweaves. Thus, the reported failure strengths of these test specimens are suspect. None of the 2-D Braids, 3-D Weaves, or thicker Uniweaves appeared to buckle during loading.

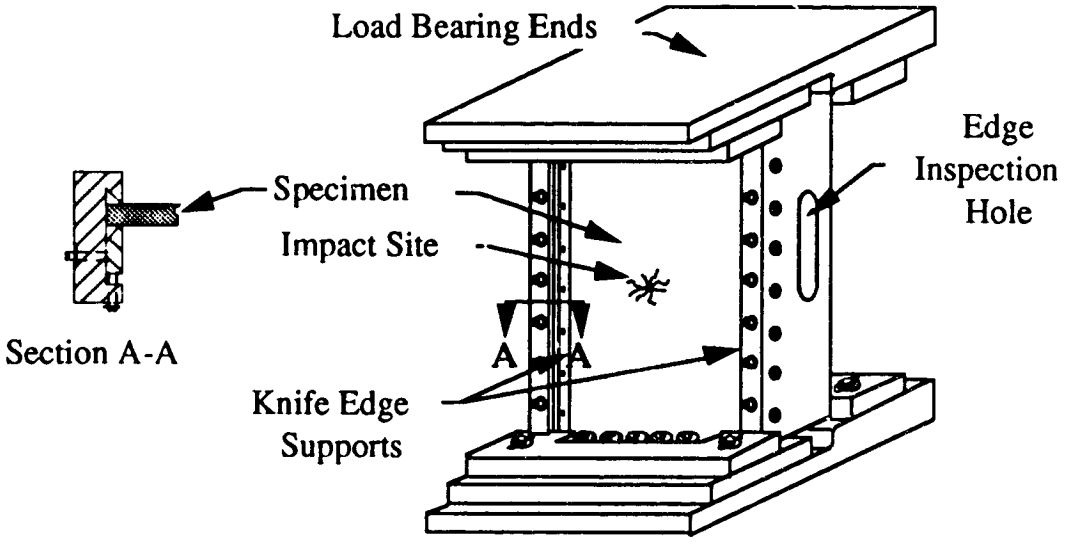

Figure 9. Compression After Impact Test Fixture Used to Prevent Global Buckling of the Specimen During Loading.

Discussion of Results

The effectiveness of textile architectures in improving damage tolerance and delamination resistance is discussed in the following sections. The initial portion of this section will discuss the damage resistance of each of the textile materials evaluated in this program. The damage measured using c-scan and the amount of impact energy required to produce this damage will be discussed. Damage tolerance, or the materials ability to support load once damaged, will be discussed next. Each of the materials is evaluated with various extents of damage and compared. The results of this study have been tabulated and are provided in Tables A1 through A7 in Appendix A.

Damage Resistance of Stitched and Unstitched Uniweaves

Damage resistance is evaluated as a function of the damage area resulting from impact and the force required to produce it. It is interesting to note that the peak impact force is directly related to the material's damage resistance. Damage initiation and growth result in a net loss of energy and reduce the impact force. This accounts for the hysteresis in the repeated loading cycles shown in Figure 6. Thus, a lower peak impact force at a given kinetic energy will typically correspond to greater damage area and lower damage resistance.

Figure 10 is a plot of damage area and impact force for both stitched and unstitched uniweaves impacted at an energy sufficient to produce Barely Visible Impact Damage. Four different specimen thicknesses are shown. Each was impacted at a different energy to produce similar dent depths. In this figure the bars represent the damage area in in^2 while the symbols indicate the peak force seen during the impact event. Each data point is an average of four specimens.

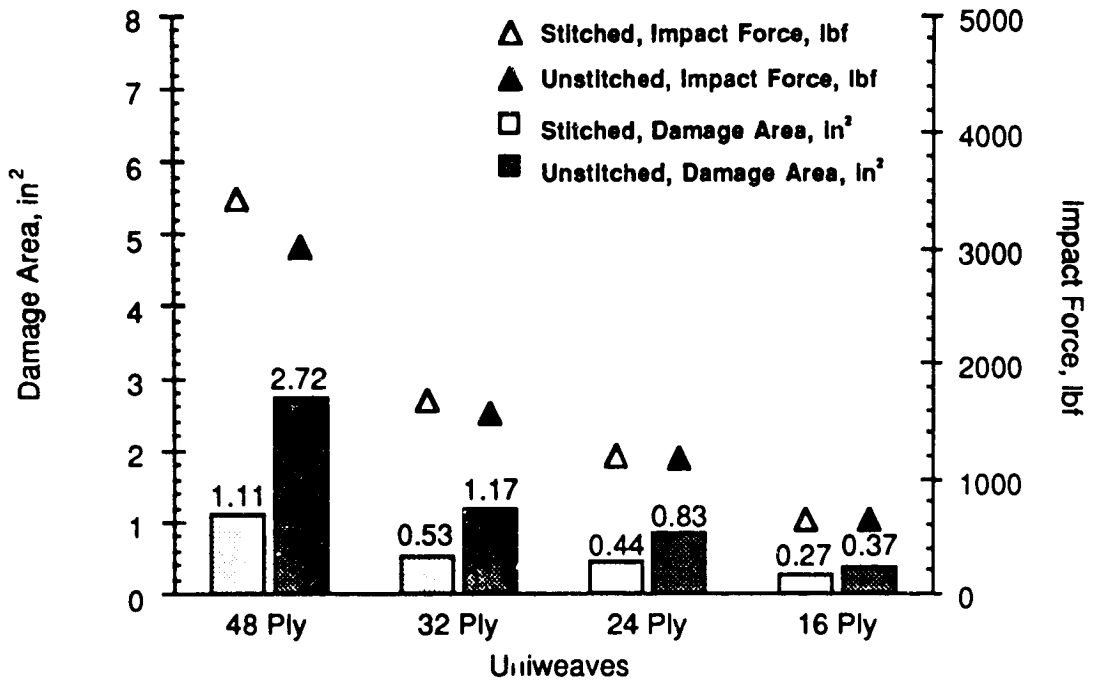

Figure 10. Damage Resistance Of Stitched And Unstitched Uniweaves Impacted At The Energy Required To Produce Barely Visible Impact Damage.

An examination of Figure 10 shows that damage area was always larger in the unstitched materials. The difference in damage area is most significant with the thicker plates. The 48 ply unstitched uniweave has almost 2.5 times the amount of damage area as the stitched 48 ply stitched uniweave. The intent was to keep the visible surface damage (dent depth) similar for each plate. The amount of impact energy required was different for each laminate. This may account for the apparent improvement in Damage Resistance with increasing plate thickness. Regardless, at each given thickness the damage area resulting from falling weight impact was less with stitching.

It is also observed in Figure 10 that for a given thickness the peak impact force obtained during the impact event is lower for the unstitched materials. Damage area tended to increase with decreasing peak force. Thus, at this energy level stitching is again shown to improve the uniweave's damage resistance.

The damage resistance of the stitched and unstitched uniweaves impact at an energy sufficient to produce Mean Impact Damage is shown in Figure 11. Damage area is represented by the shaded bars and impact force is shown with the open and filled symbols. The data points are averages of four separate experiments.

Figure 11 shows that damage resistance continues to be improved by stitching. The damage areas are significantly smaller and peak impact energies are significantly higher in all cases for the stitched laminates. An apparent effect of plate thickness is also shown in the data. As the plate thickness increases, so does the percentage improvement in damage resistance. The 48 ply unstitched uniweave has 2.8 times more damage area than the stitched 48 ply uniweave.

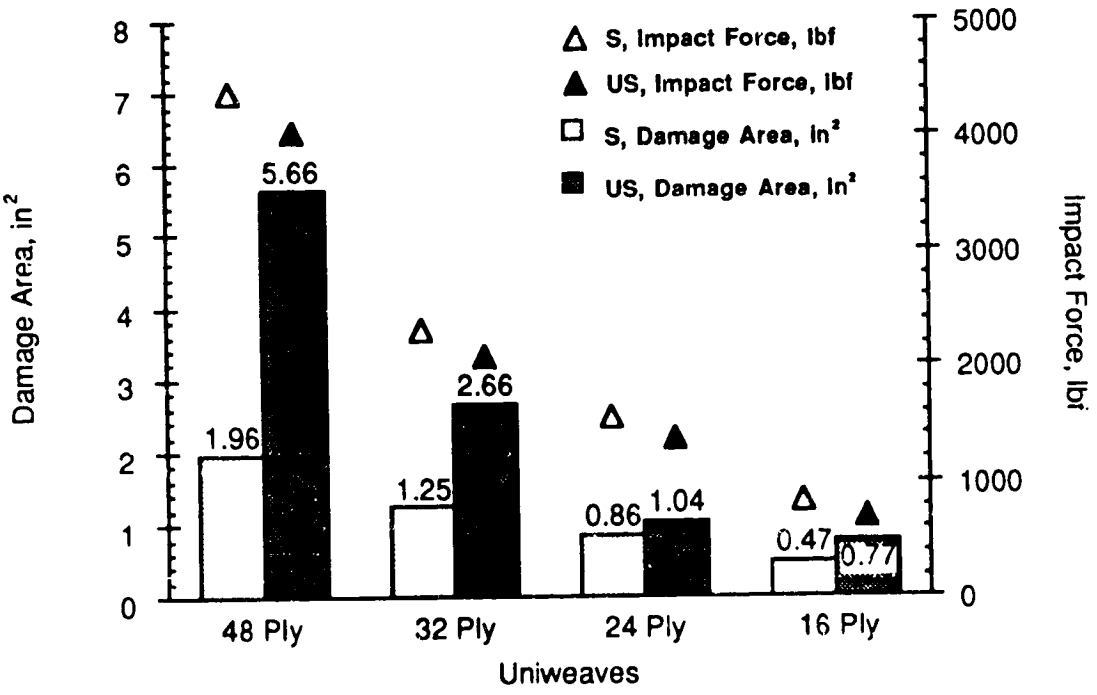

Figure 11. Damage Resistance Of Stitched And Unstitched Uniweaves Impacted At The Energy Required To Produce Mean Impact Damage.

Figure 12 shows the response of the stitched and unstitched uniweave to a severe impact. These specimens were impacted at an energy sufficient to produce Visible Impact Damage. This level of impact energy was sufficient to produce a surface dent with an average depth of 0.10 in. Damage area and impact force for each of the four ply thicknesses are shown. In this figure the bars represent the amount of damage area while the symbols indicate the peak force seen during the impact event. Four experiments were averaged for each data point shown.

Stitching continues to improve the uniweaves' damage resistance. Damage areas are smaller and peak impact energies are higher for the stitched materials in all cases. Comparing this figure to the Barely Visible Impact energy level shown in Figure 10 reveals that damage area increased almost 300% in the unstitched materials but only about 200% with the stitched uniweaves as impact energy increased. The benefit of stitching is more pronounced with the thinner plates at the VID impact level while the opposite was true at the mean and BVID impact energy levels. Thus, stitching continues to improve damage resistance even at the severe impact energy levels.

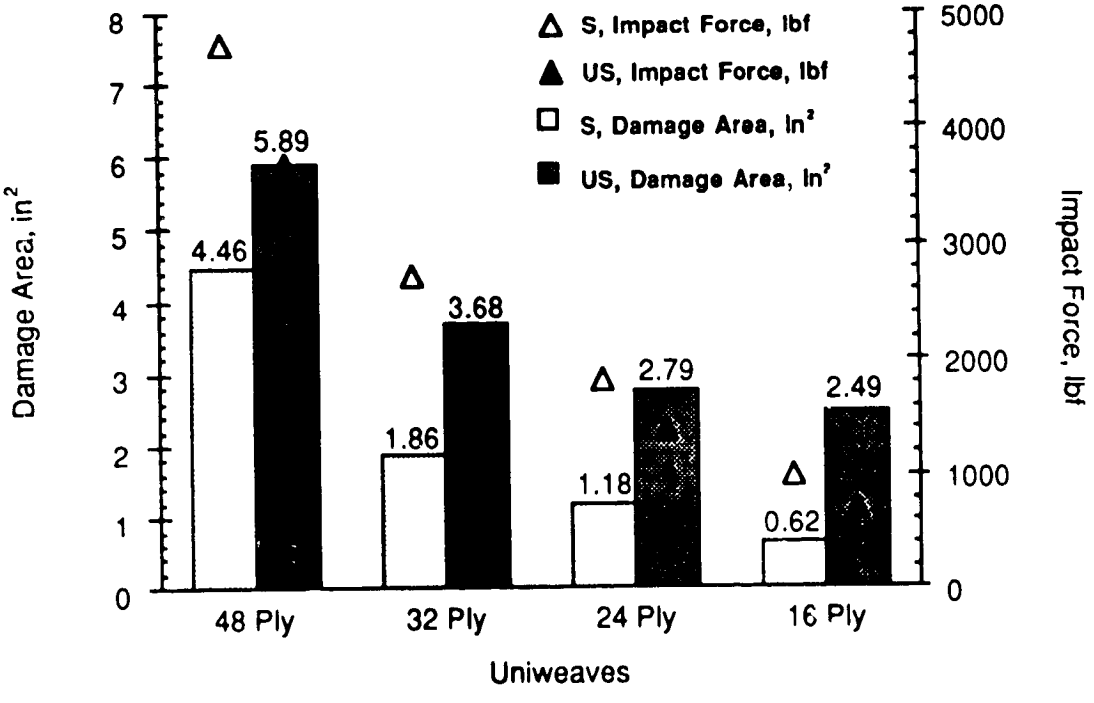

Figure 12. Damage Resistance Of Uniweaves Impacted At The Energy Required To Produce Visible Impact Damage.

The damage resistance of each of the 2-D braids and 3-D weaves is compared in the following figures. Again comparisons are based on the damage areas calculated from c-scans and the peak impact force.

Figure 13 is a plot of damage area and impact force for each of the 2-D braids. The specimens were impacted at an energy sufficient to produce Barely Visible Impact Damage. Damage area is represented by the bars; peak impact force is represented by the symbols. Each data point is an average of four specimens.

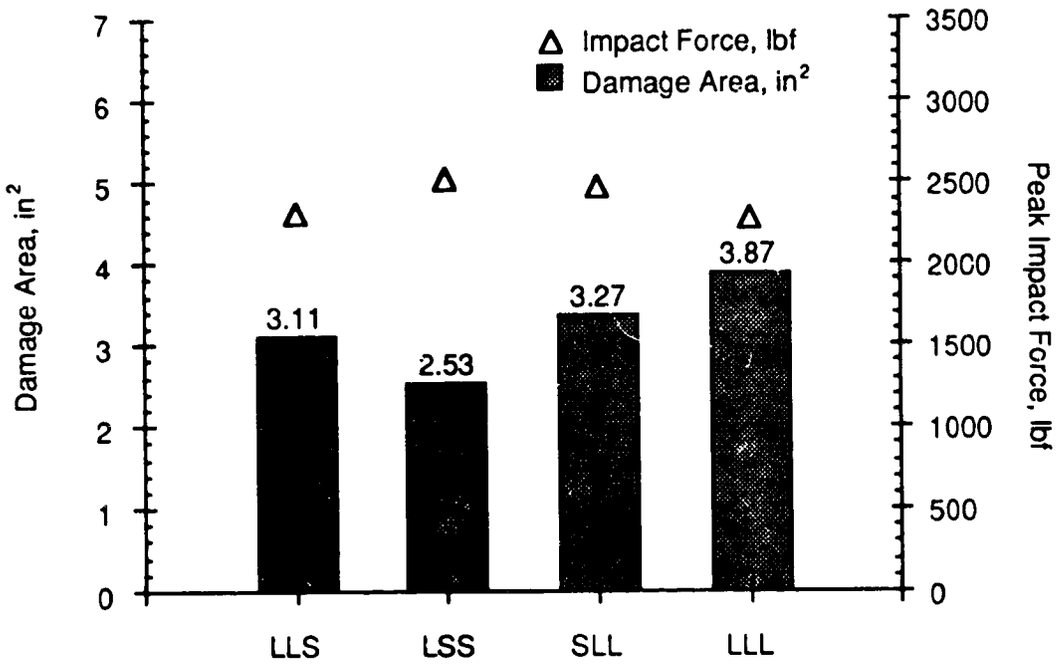

Figure 13. Damage Resistance Of 2-D Braids Impacted At 15.39 Ft•Lbf. To Produce Barely Visible Impact Damage.

An examination of Figure 13 shows that all of the 2-D braids suffered significant amounts of damage at this level of impact energy. A review of the data in Figure 10 indicates that the stitched uniweaves with a similar thickness (48 ply ≈ 0.25 in.) had only 1.11 $in.^2$ of damage area. Even the unstitched uniweaves, with only 2.72 $in.^2$ of damage area, tolerated the BVID impact event better than the 2-D braids. This result suggests that the braids are not as resistant to impact induced damage as the uniweave materials.

Damage resistance of the 2-D braids impacted at an energy sufficient to produce Visible Impact Damage is shown in Figure 14. All four braid types are compared and each data point is an average of three experiments. The shaded bars represent the damage area while peak impact force is given by the open symbols. Each data point is an average of four specimens.

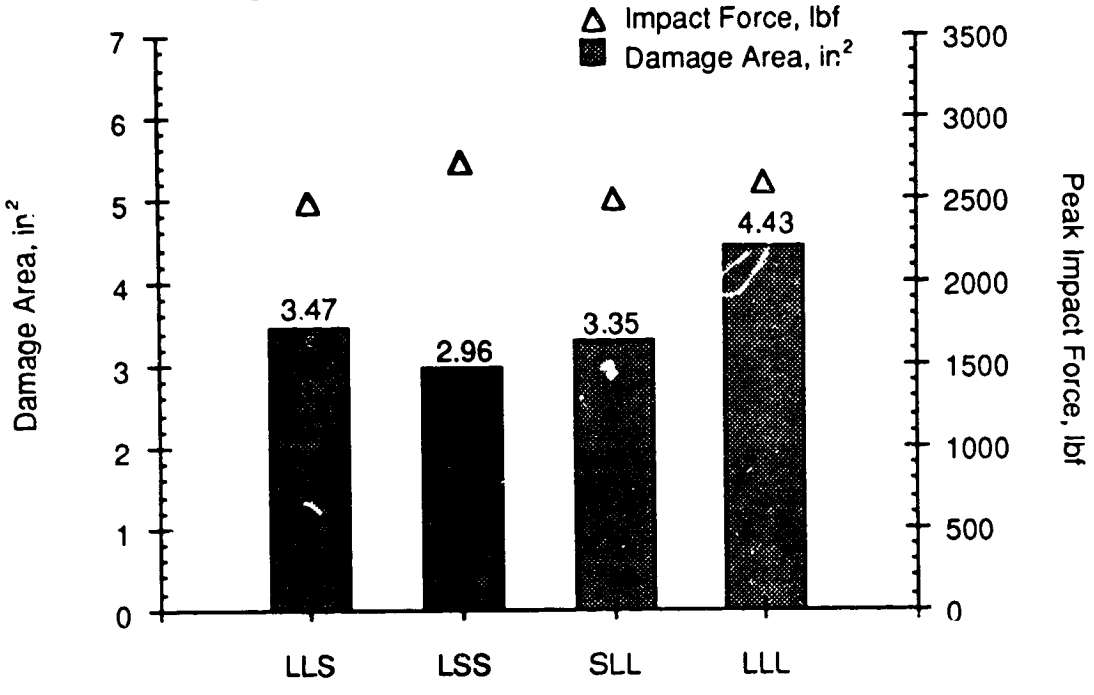

Figure 14. Damage Resistance Of 2-D Braids Impacted At 62.86 Ft•Lbf. To Produce Visible Impact Damage.

A comparison of the data shown in Figure 14 with those in Figure 13 shows that, although damage areas were large as compared with the other material forms, damage area increased only 11% between the BVID and VID energy levels.

Varying the braiding parameters produced little in the way of significant improvements in damage resistance. The LSS architecture, which contained the smallest tow size, did show the most resistance to damage growth but the extent of damage was still fairly severe. The SLL and LLL architectures are the same with the exception of their fiber bundle size. The SLL used 30k tows while the LLL used 75k tows. Damage area increased 32 percent between these two materials at this impact energy but only 18 percent at the lower BVID energy. At both impact levels, the SLL had the least measurable damage area. This suggests that smaller tow size may

result in improved damage resistance at the more severe impact levels.

Figure 15 is a plot of damage area and impact force versus each material type for five of the 3-D weaves investigated. The specimens were impacted at the Barely Visible Impact Damage level. Data for the OS2 material is not reported due to the inability to acquire c-scan data on this material form. The shaded bars represent the damage area and the symbols indicate the peak impact force. Each data point represents the average of four experiments.

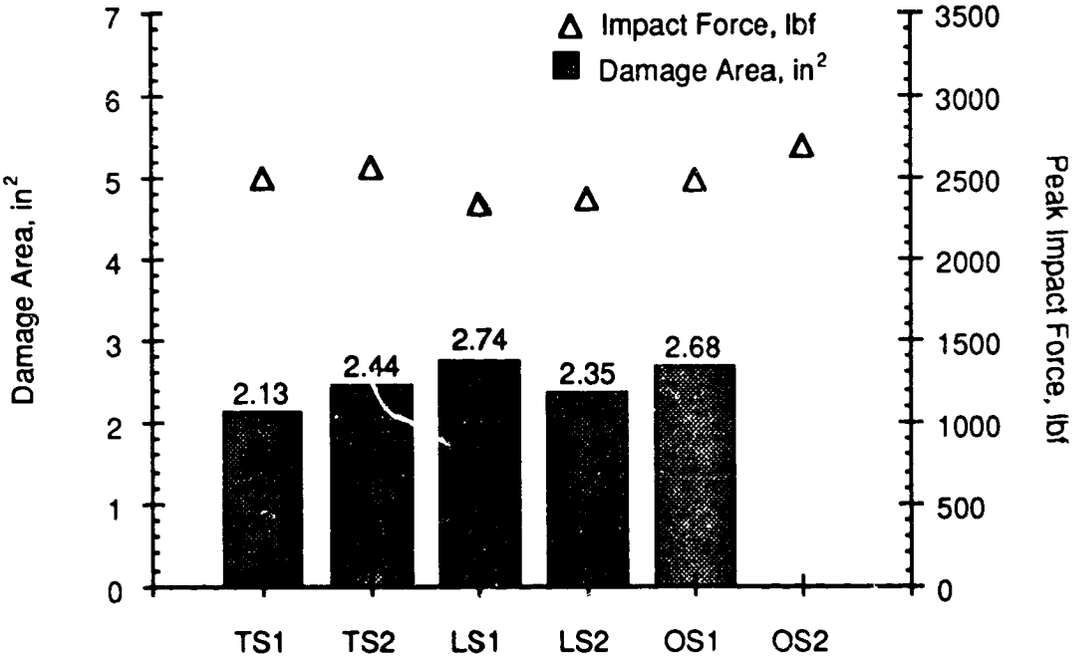

Figure 15. Damage Resistance Of 3-D Weaves Impacted At 15.39 Ft•Lbf. To Produce Barely Visible Impact Damage.

At this impact energy, damage resistance was improved over the 2-D braids and unstitched uniweaves but not over the stitched uniweaves. All the 3-D weaves appeared to respond to the BVID impact in a similar fashion. The standard deviation of the measured damage areas shown in the figure was less than 0.25 in^2.

The OS2 material had the largest peak impact force. This suggests that damage area may have been small in these specimens. It will later be shown that the OS materials are the most damage tolerant of the 3-D weaves.

Recall that the "1" materials have yarn bundles twice as large as the "2" materials. An examination of these data shows that increasing the tow size had no consistent effect on damage resistance.

The damage resistance of the 3-D weaves impacted at the Visible Impact Damage level is compared in Figure 16. Damage area and impact force are shown for five of the six weaves evaluated in this study. Again the OS2 damage area data is missing due to the inability to acquire c-scan data on this material form. Each data point is an average of four specimens.

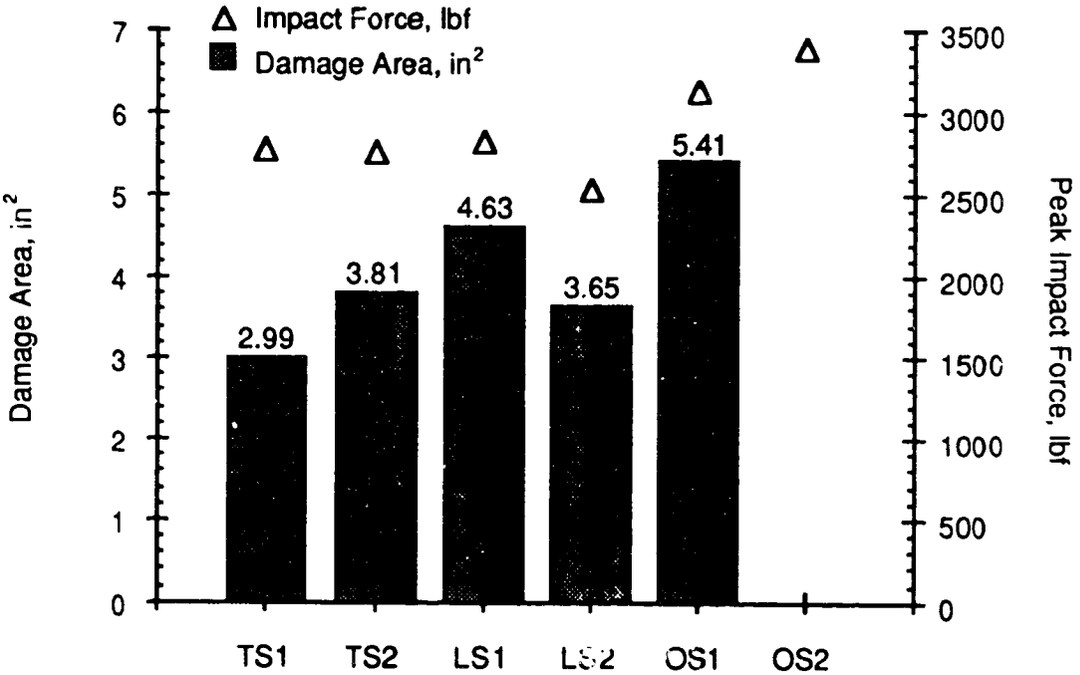

Figure 16. Damage Resistance Of 3-D Weaves Impacted At 62.86 Ft•Lbf. To Produce Visible Impact Damage.

Damage resistance was improved over the unstitched uniweaves but not over the 2-D braids or stitched uniweaves at this impact energy. There was a 64% average increase in damage area between the BVID and VID impacts. The OS2 specimen again had the highest peak impact force while the OS1 displays the largest measured damage area. There also appears to be an improvement in damage resistance with the through-the-thickness angle interlock materials. It will later be shown that this trend reverses itself in a comparison of the damage tolerance of the TS and OS architectures.

As with the BVID data, no consistent improvement was found among the "1" and "2" materials. There was however a trend among the similar materials impacted with different energies. At both energies the TS1 has less damage area than the TS2 while the LS1 has more damage area than the LS2. This suggests that tow size effects may be architecture dependent .

Damage Tolerance of Stitched and Unstitched Uniweaves

Damage Tolerance is defined as a materials ability to support load after being damaged. Compression after impact and tension after impact strengths were used as a discriminator of the damage tolerance in this investigation. Evaluations will be made comparing both strength and residual strength where residual strength is the post-impact strength normalized by its unnotched strength.

Damage Tolerance in Compression

Figures 17 and 18 show an evaluation of the compression response of the stitched & unstitched uniweaves that have been impacted at the lower Barely Visible Impact Damage energy levels. Figure 17 is a plot of the compression after impact (CAI) strength for each of the material forms. The CAI data, normalized by their respective unnotched strengths, are reported in Figure 18. Each data point is an average of two experiments. Noticeable bending was present in the 16 ply and some 24 ply specimens during loading. Thus, the failure strengths for these experiments may be low.

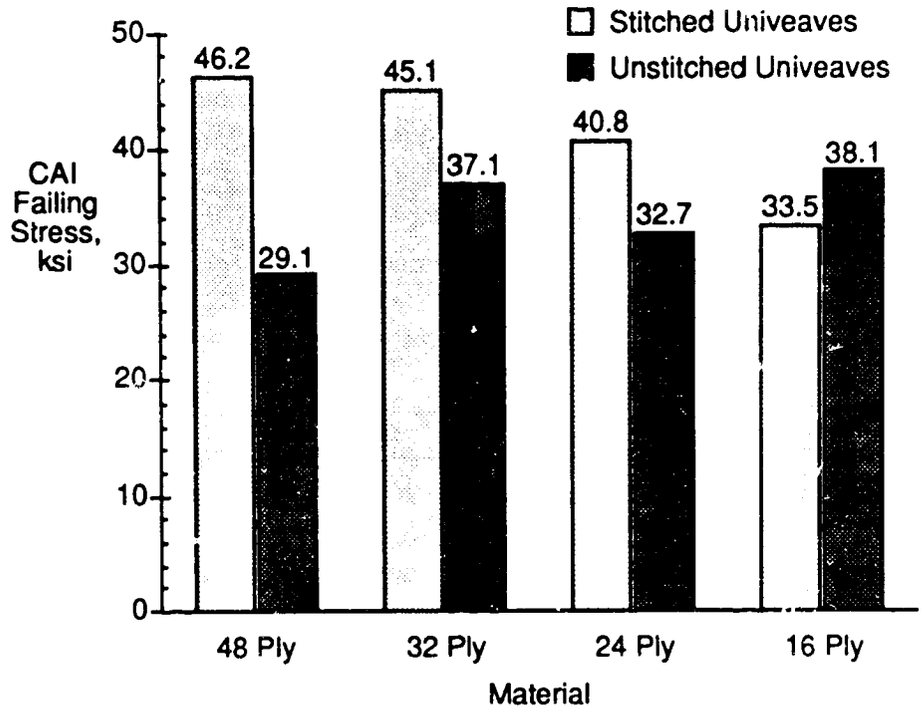

Figure 17. Compression-After-Impact Strength Of Stitched And Unstitched Uniweaves Impacted At The Energy Required To Produce Barely Visible Impact Damage.

A review of the data indicates that, with the exception of the 16 ply specimens, compression strengths were improved with stitching. The strengths of the 16 ply stitched specimens were probably lower than their unstitched counterparts due to bending. The data also indicates that the stitched laminates' compression strength exceeded 40 ksi, a current industry target for CAI strength, in three of the four case. The 16 ply specimens were, again, the lone exception. The compression strengths of the unstitched laminates averaged only 34 ksi.

In general, stitching appears to enhance this material's damage tolerance. The stitched laminates' residual strength increases with increasing plate thickness. For example, the 48 ply stitched laminates averaged more than 93% strength retention while the 24 ply stitched uniweave retained only 83 percent.

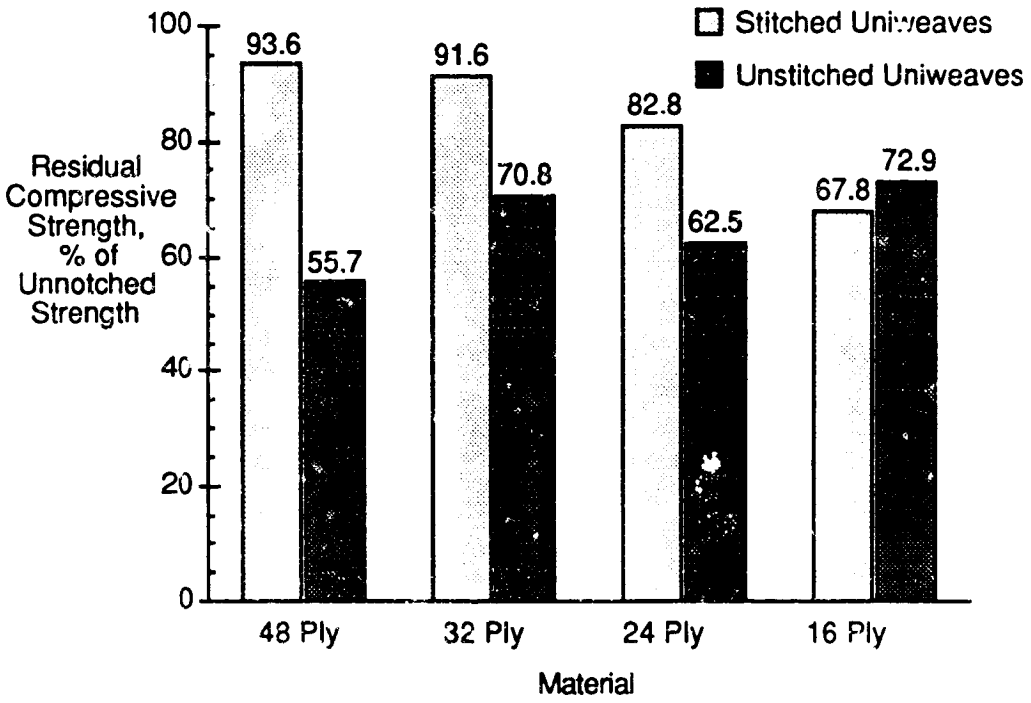

Figure 18. Damage Tolerance Of Stitched And Unstitched Uniweaves Impacted At The Energy Required To Produce Barely Visible Impact Damage.

The compression response of the stitched & unstitched uniweaves, impacted at the higher Visible Impact Damage energy levels, are shown in Figures 19 and 20. Figure 19 is a plot of the compression after impact (CAI) strength for each of the material thicknesses and Figure 20 is a plot of the residual strengths where the CAI data has been expressed as a percentage of unnotched strength. Each data point is an average of two experiments.

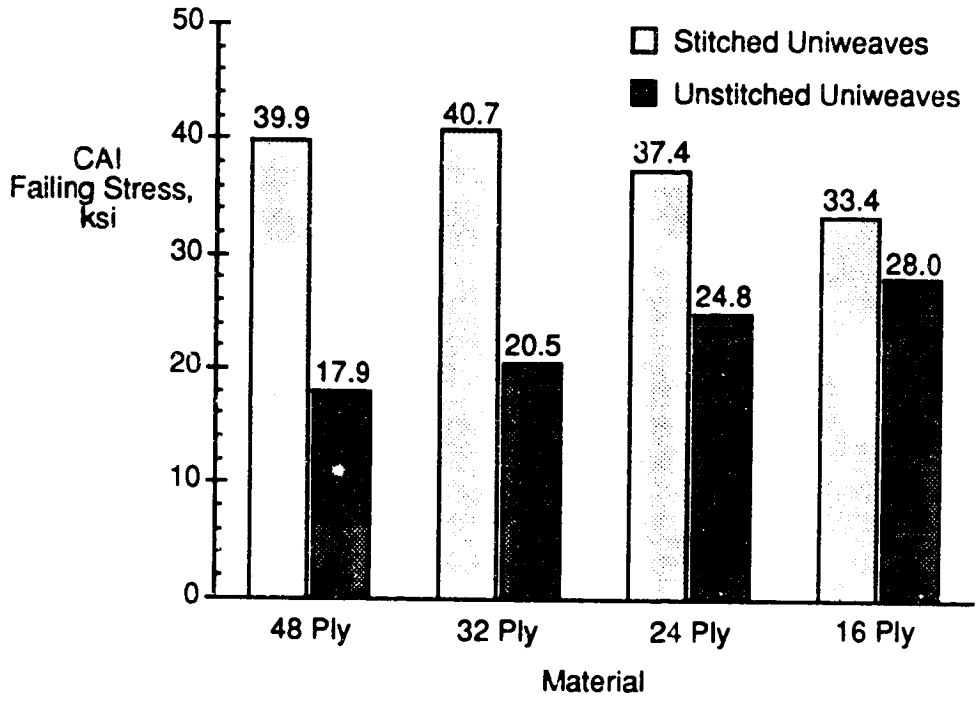

Figure 19. Compression Strength Of Stitched And Unstitched Uniweaves Impacted At The Energy Required To Produce Visible Impact Damage.

Stitching continues to enhance the damage tolerance with more severe damage. The difference in CAI strength with and without stitching appears to be more significant at this higher impact energy. A review of Figure 17 data shows that the CAI strength of the 48 ply material was improved 59% with stitching. At this higher VID impact energy, the CAI strength of the 48 ply stitched uniweave is 123% greater than the unstitched uniweave. Thus, the effectiveness of stitching increases with increasing impact energy.

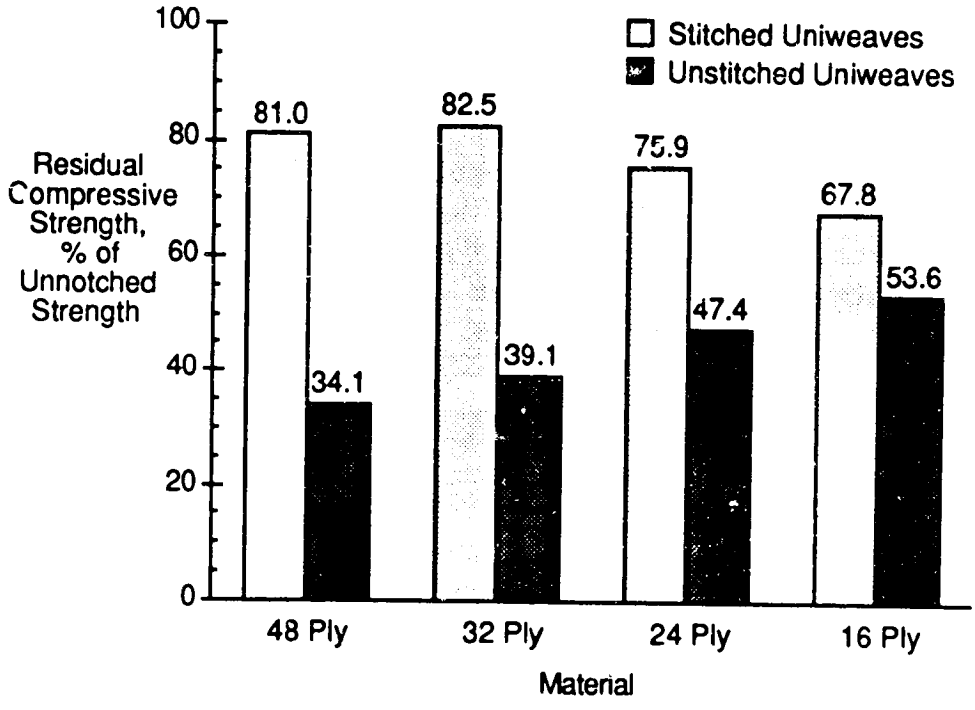

Figure 20. Damage Tolerance Of Stitched And Unstitched Uniweaves Impacted At The Energy Required To Produce Visible Impact Damage.

Again, damage tolerance with stitching tended to improve with increasing plate thickness. Residual strengths were around 80% of the unnotched strength for the thicker 48 and 32 ply specimens but dropped to 76% and 68% for the 24 and 16 ply laminates. This result may be an artifact of the specimen buckling. Even at this severe impact energy level, compression strengths were around the 40 Ksi target. The stitched laminates averaged about 38 ksi.

Damage Tolerance in Tension

Figure 21 and 22 show an evaluation of the tension response of the stitched and unstitched uniweaves impacted at the lower Barely Visible Impact Damage energy level. Figure 21 is a plot of the tension after impact (TAI) strength. Figure 22 is a plot of the residual strength where the TAI data for each thickness has been normalized by its unnotched tensile strength. Two experiments were averaged for each data point shown.

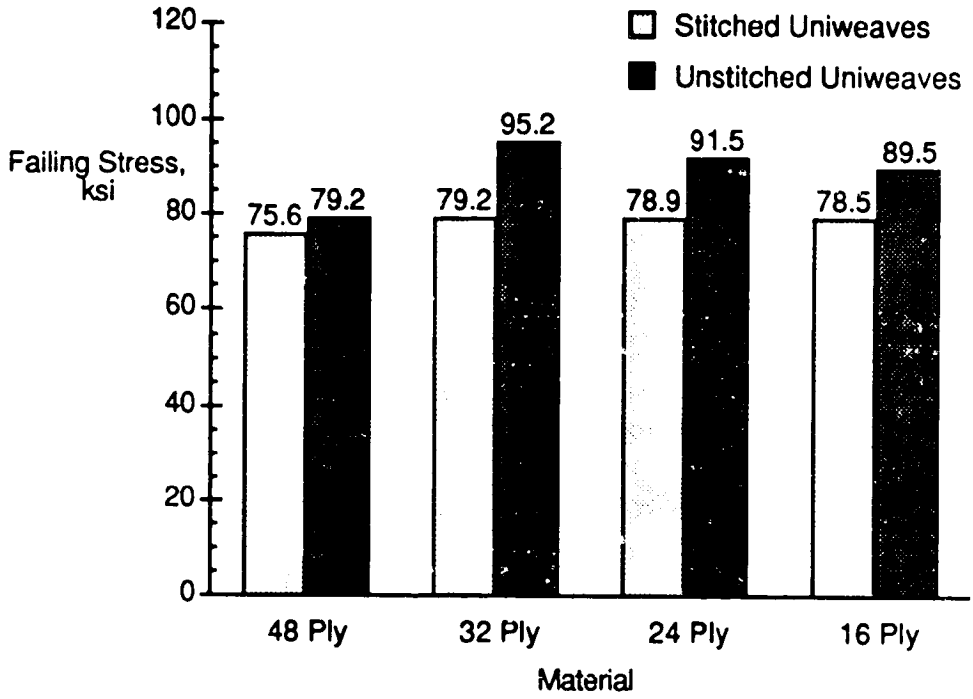

Figure 21. Tension Strength Of Stitched And Unstitched Uniweaves Impacted At The Energy Required To Produce Barely Visible Impact Damage.

An examination of Figures 21 and 22 shows that stitching doesn't appear to enhance the tension after impact strength. Some improvement to the residual tensile strength is apparent but may be due to low unnotched strength. It's important to realize that because of the stitch yarns, the stitched uniweaves were slightly thicker than the unstitched laminates. Because stress is calculated based on specimen thickness, and tension strength in composites is 0° fiber dominated, the stitched uniweaves tended to have slightly lower load carrying capability in tension than the unstitched uniweaves.

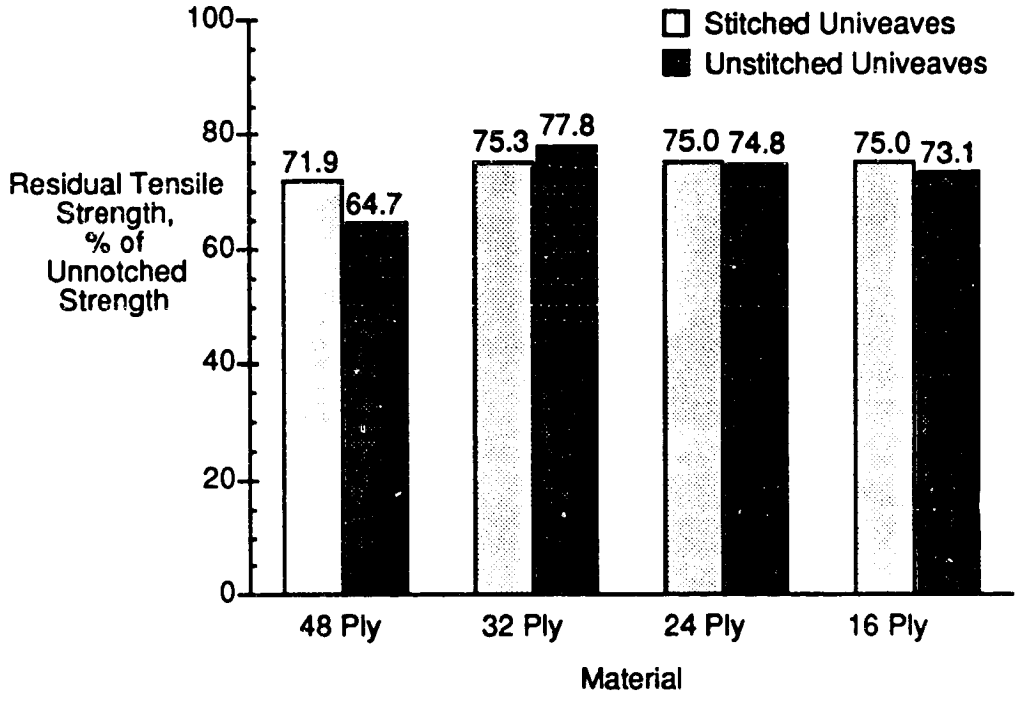

Figure 22. Damage Tolerance Of Stitched And Unstitched Uniweaves Impact At The Energy Required To Produce Barely Visible Impact Damage.

The stitched uniweaves had an average failure strength of 78 ksi and an average of 74% strength retention while the unstitched averaged 89 ksi failure strength and only a 73% retention of unnotched strength. Thus, even though the failure strengths were lower, the percent retention of residual strengths was about equal.

E. amination of Figures 21 and 22 show little effect of plate thickness on the failure stress or residual strength of these materials at this impact energy level.

Some of the uniweaves were impacted at a "mean" energy level. The response of the uniweave to this intermediate impact energy is given in Figures 23 and 24. Figure 23 is a plot of the tension after impact strength for each of the four uniweaves and Figure 24 is a plot of the data expressed as a percent of its unnotched strength. Each data point is an average of two experiments.

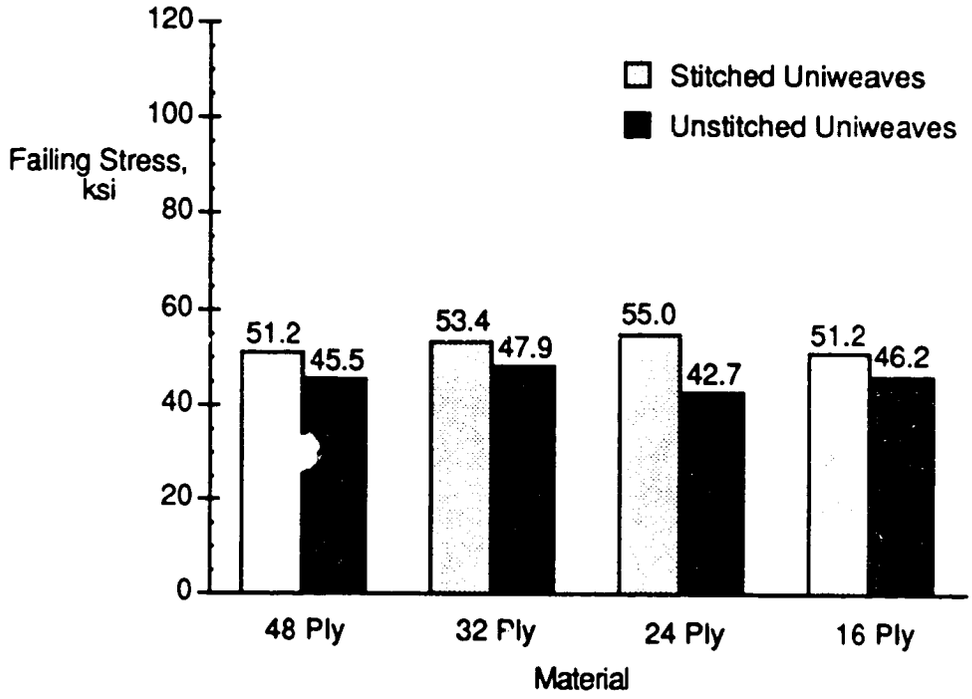

Figure 23. Tension Strength Of Stitched And Unstitched Uniweaves Impact At The Energy Required To Produce Mean Impact Damage.

At this median value of impact energy, stitching tended to improve the damage tolerance of the uniweaves. At all ply counts, failing stresses were greater for the stitched laminates.

Strengths with mean impact damage were significantly lower than those obtained at the BVID impact energy. Examination of the data in Figure 21 shows that the stitched uniweaves had an average tensile strength of 78 ksi after a BVID impact. The average strength of the stitched laminates shown in Figure 23 was 53 ksi. This is a 48 % reduction in average strength as a result of the increased impact energy. The unstitched uniweaves averaged 89 ksi with BVID impact and 46 ksi at the "mean" impact energy. This is a 95% decrease in strength as a result of the increase in impact energy. Thus, the sensitivity to impact damage in tension is strongly dependent on the level of damage.

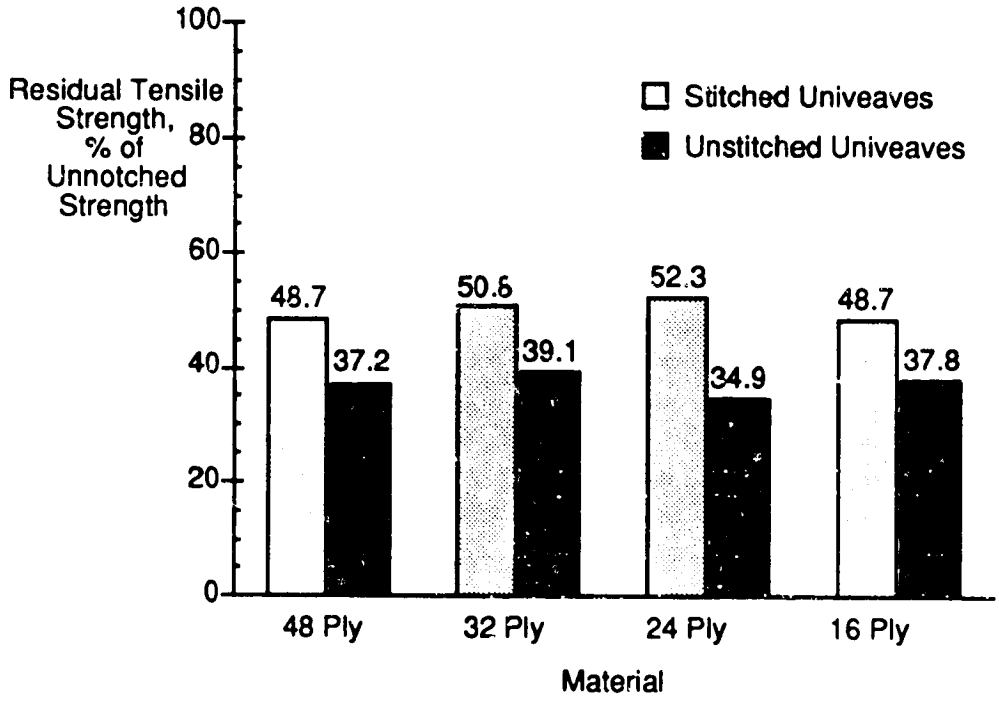

Figure 24. Damage Tolerance Of Stitched And Unstitched Uniweaves Impacted At The Energy Required To Produce Mean Impact Damage.

Improvements in strength resulting from stitching seem to improve with increasing damage. The percentage of residual strength retention was larger at this higher impact energy level. The stitched and unstitched laminates both averaged about 74 percent strength retention with BVID impact. At the mean impact energy, the stitched uniweave averaged a 50% retention of their unnotched strength while the unstitched laminates average fell to 37%.

Damage tolerance of the stitched and unstitched uniweaves to impact at the higher Visible Impact Damage energy level is shown in Figures 25 and 26. Two experiments were averaged for each data point. Figure 25 is a plot of the tension after impact strength for each of the uniweaves. Residual strength retention, shown as a percentage of the unnotched strength, is given in Figure 26 for each of the specimens.

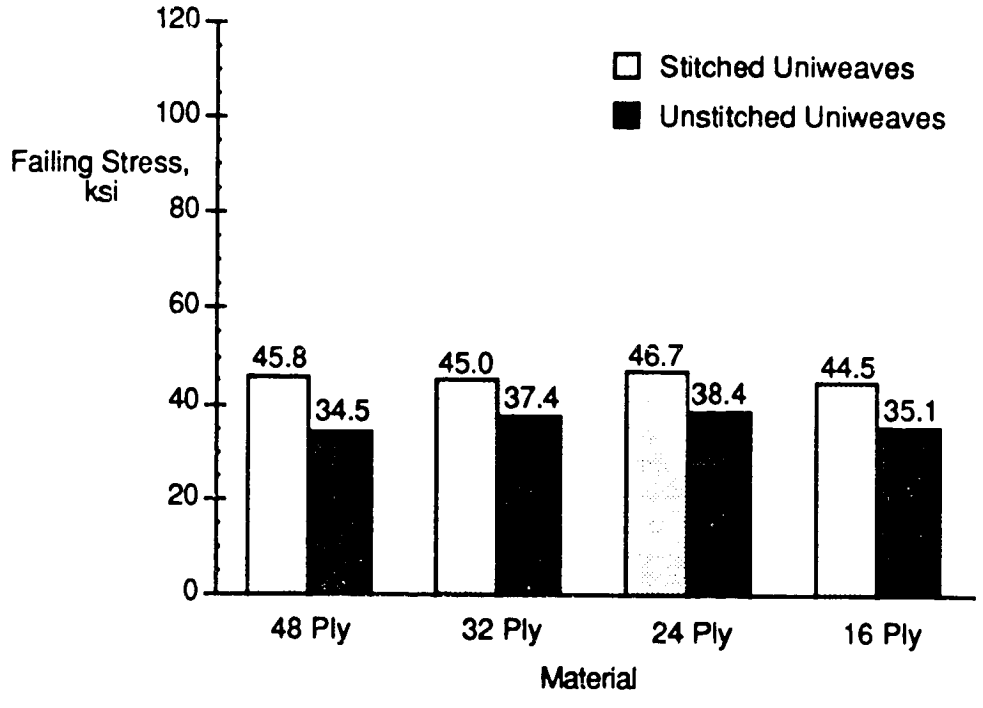

Figure 25. Tension Strength Of Stitched And Unstitched Uniweaves Impacted At The Energy Required To Produce Visible Impact Damage.

Stitching also moderately improves the damage tolerance of the uniweaves with severe impact. Failing stresses were again greater for the stitched uniweaves than for the unstitched materials. Failure stresses were all above 40 ksi for the stitched specimens but averaged only 36 ksi for the unstitched.

Although stitching has improved the uniweaves TAI strength, the stitched laminate strengths have been reduced to around 43 percent of their unnotched value by the VID impact. Recall the data in Figure 20, a plot of the residual strength of the compression after impact response of the uniweaves at the VID impact energy. Strength retention averaged approximately 80 percent of its unnotched value in compression. Thus, improvements in damage tolerance are not as significant in tension as they are in compression.

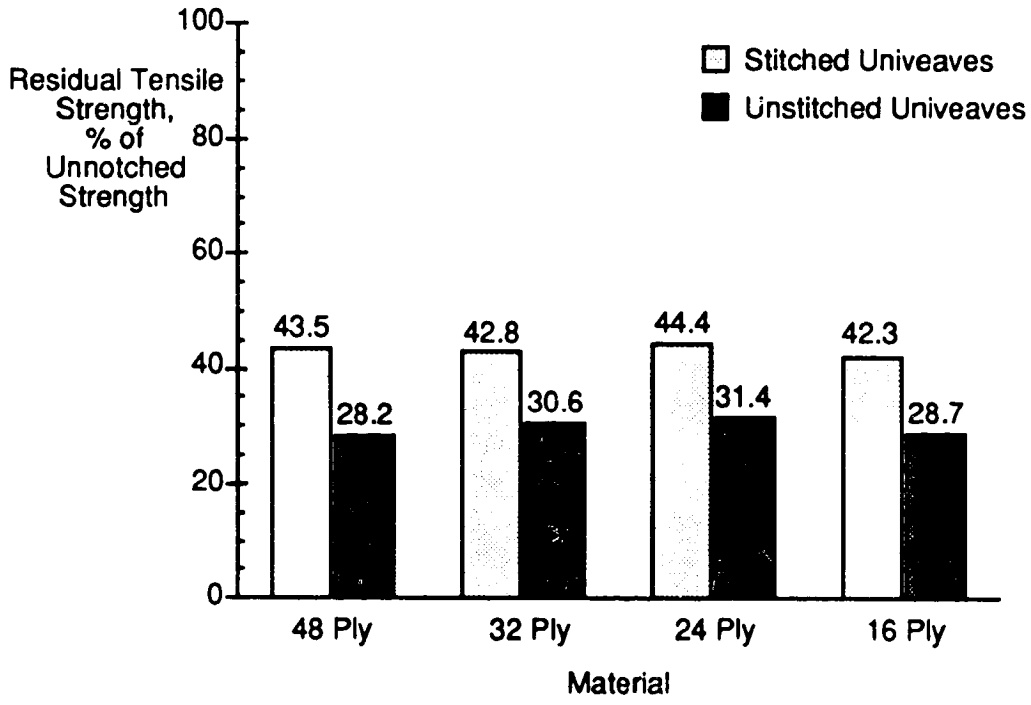

Figure 26. Damage Tolerance Of Stitched And Unstitched Uniweaves Impacted At The Energy Required To Produce Visible Impact Damage.

Damage tolerance of the 2-D braids and 3-D weaves are shown in the following figures. Again the compression after impact (CAI), tension after impact (TAI), and residual strength of each will be used to make the comparisons. Each figure shows results from both the Barely Visible Impact Damage impact energy of 15.39 ft•lbs and the Visible Impact Damage impact energy of 62.86 ft•lbs. Because the braids differed only in architecture, not thickness, impact energy was kept constant between material types.

Compression after impact (CAI) strength is plotted in Figure 27 while residual strength, expressed as a percentage of the unnotched strength, is shown in Figure 28 for each of the four 2-D Braided architectures. Data for both the lower Barely Visible Impact Damage level and the upper Visible Impact Damage level are shown in each figure. Each data point is an average of two experiments.

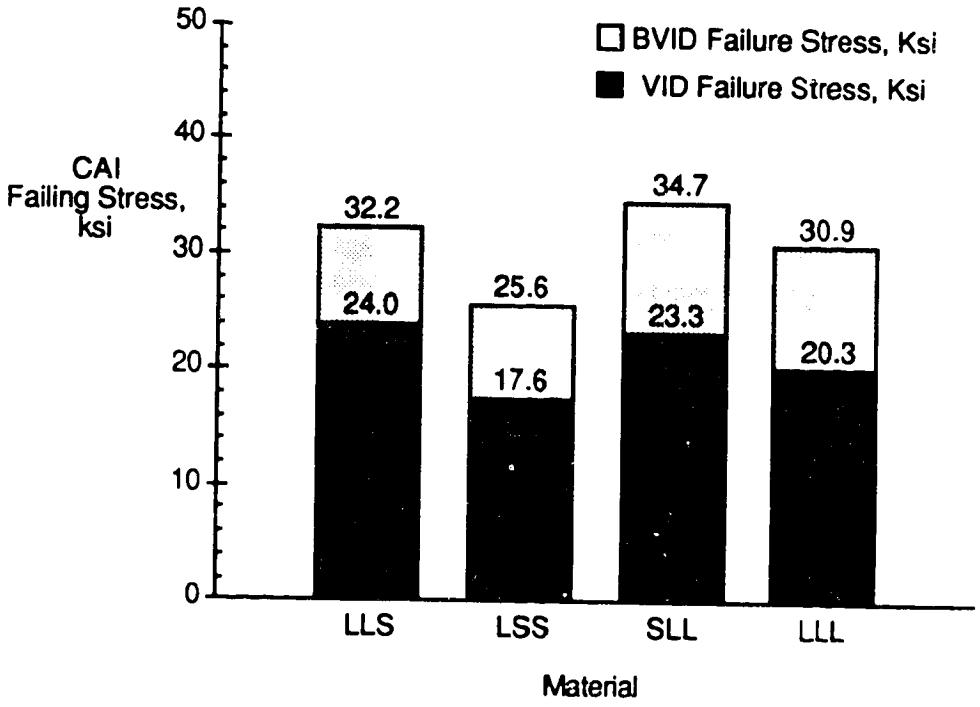

Figure 27. Compression Strengths of 2-D Braids with BVID (15.39 ft•lbs) and VID (62.86 ft•lbs).

An examination of Figures 27 and 28 shows that the strength of the 2-D braids are significantly reduced by impact damage. None of the 2-D braids retained more than 63% of their unnotched strength.

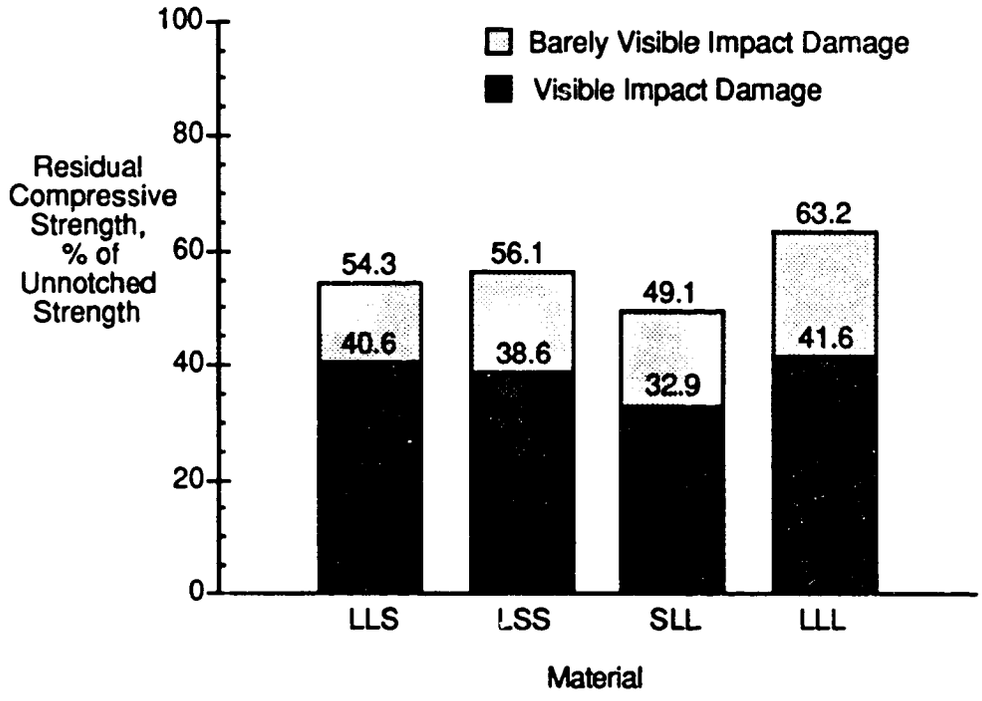

Figure 28. Damage Tolerance of 2-D Braids with BVID (15.39 ft•lbs) and VID (62.86 ft•lbs).

Recall that some of the braids were designed to allow an evaluation of tow size effects. Specifically, the SLL and LLL architectures were constructed exactly the same with the exception of tow size. The LLL contains tow bundles 2.5 times the size of the SLL. An examination of the impact response of these two material architectures shows some interesting effects. Strengths were greater for the SLL material, regardless of impact energy level. Thus it would seem that the smaller tow size in the SLL material must contribute to a strength improvement. Notice, however, that in Figure 28, the residual strength ratio of the LLL braid is better than that of the SLL material. Therefore, the increase in tow size decreased the unnotched strength of the material more than the CAI.

Figure 29 is a plot of the tension after impact (TAI) response of each of the 2-D braids. Data for both the BVID and VID impact energy levels are given. Data shown are averages for two experiments.

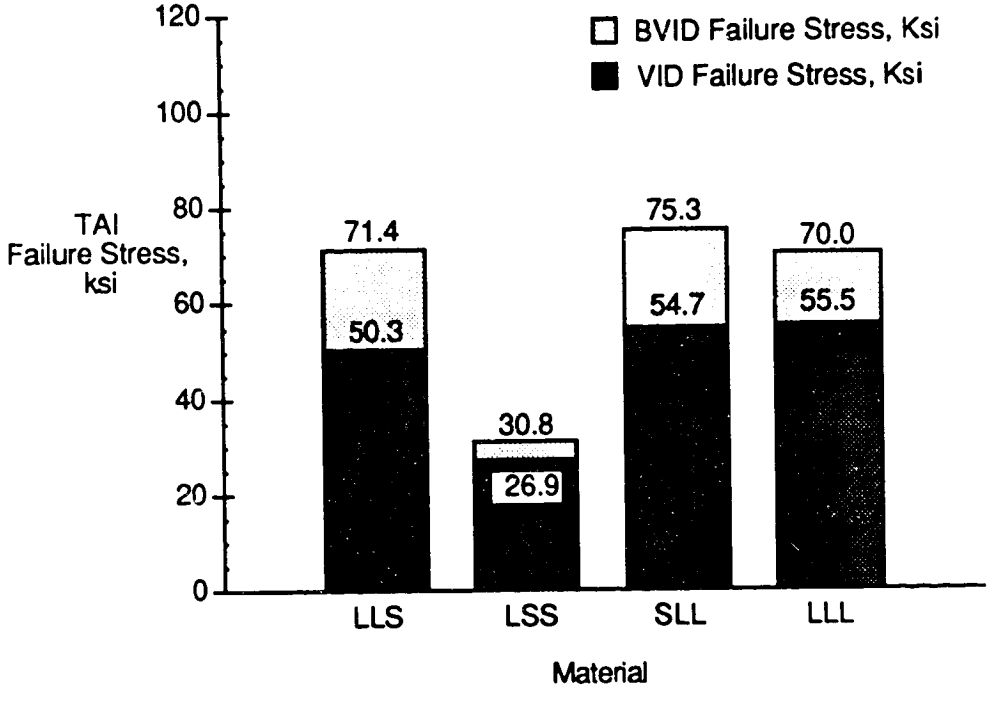

Figure 29. Tension Strength of 2-D Braids with BVID (15.39 ft•lbs) and VID (62.86 ft•lbs).

Examination of Figure 29 shows the 2-D braids response to impact damage is better in tension than in compression. With the exception of the LSS material, strengths averaged above 72 ksi with Barely Visible Impact Damage and above 53 ksi with Visible Impact Damage. Recall that the LSS has only 12% axial yarns. This accounts for its significantly lower failure stress.

Residual Strength as a percentage of unnotched strength is plotted in Figure 30 for each of the four 2-D Braided architectures. Data for both the lower Barely Visible Impact Damage level and the upper Visible Impact Damage level are shown in this figure. Data shown are averages for two experiments.

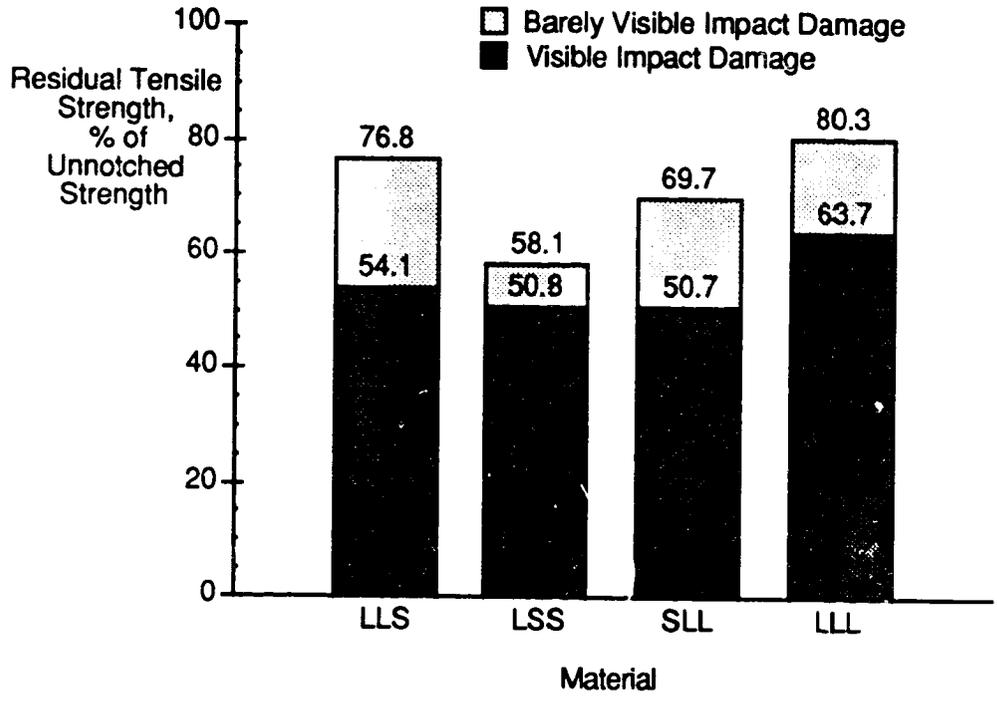

Figure 30. Damage Tolerance of 2-D Braids with BVID (15.39 ft•lbs) and VID (62.86 ft•lbs).

The LLL again has the greatest percentage retention of unnotched strength. At the Visible Impact Damage impact energy, the average percent residual strength is only 16% less than at the lower BVID impact energy level. Although the 2-D Braids performed significantly better in tension than in compression, their overall strength retention is still rather low. An examination of tow size effects in tension reveals a response similar to that found in compression with these materials. The SLL has somewhat higher strength but a lower strength retention percentage than the LLL material.

Compression after impact (CAI) strength is plotted in Figure 31 and residual strength as a percentage of unnotched strength is shown in Figure 32 for each of the six 3-D weaves tested. Data from both the lower Barely Visible Impact Damage level and the upper Visible Impact Damage level are shown in each figure. Data shown are averages for two experiments.

The data indicate that the weaves outperformed the 2-D braids and the unstitched uniweaves at both impact energy levels in compression. The woven laminates compared about equally with the stitched uniweaves; the OS2 material had a failing stress of greater that 40 ksi at the highest impact energy.

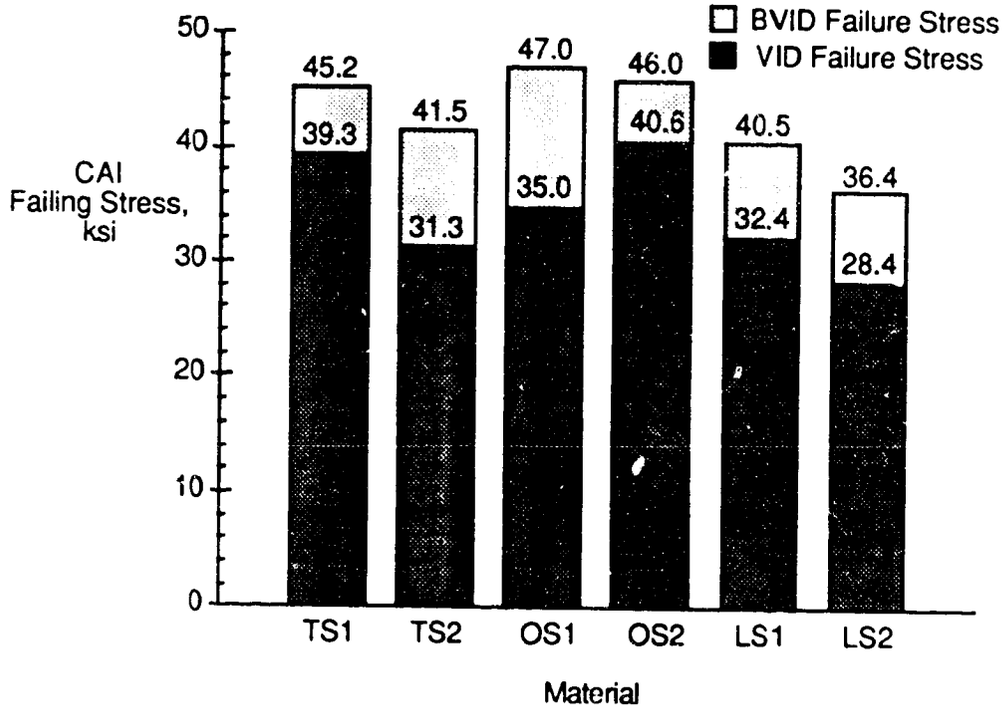

Figure 31. Compression Strength of 3-D Weaves with BVID (15.39 ft•lbs) and VID (62.86 ft•lbs).

The data also indicate that the woven materials' residual strengths (expressed as a percentage of their un-impacted compression strengths) were better that those of the 2-D Braids regardless of the impact energy level. The unstitched uniweaves retained a higher percentage of their unnotched strength than the 3-D weaves at the lower impact energy level but not at the more severe VID level. However, the Stitched Uniweaves outperformed the 3-D Weaves in compression, regardless of the impact energy level.

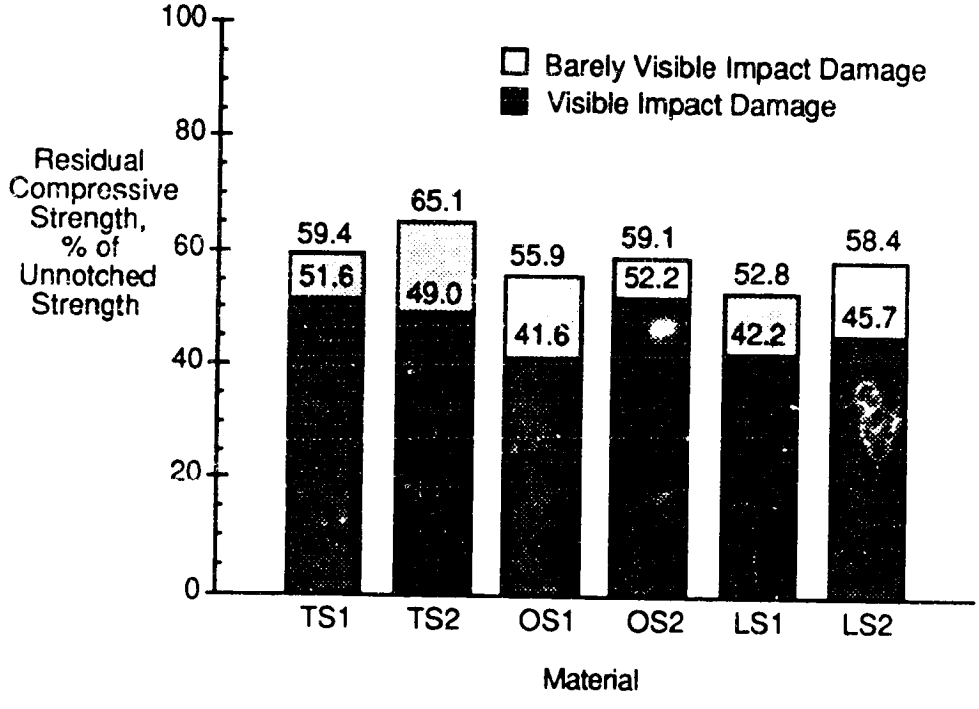

Figure 32. Damage Tolerance of 3-D Weaves with BVID (15.39 ft•lbs) and VID (62.86 ft•lbs).

The 3-D weaves were constructed in pairs. The "1" materials had yarn bundles twice as large as the "2" materials. Although the specimens made of the larger yarns had slightly greater compression strengths after being impacted at the BVID level, no consistent pattern was evident in the materials impacted at the more critical VID level.

The tension after impact response of the 3-D weaves is shown in Figure 33. Data from both the lower Barely Visible Impact Damage level and the upper Visible Impact Damage level are shown in each figure. Averages from two experiments are represented by each data point.

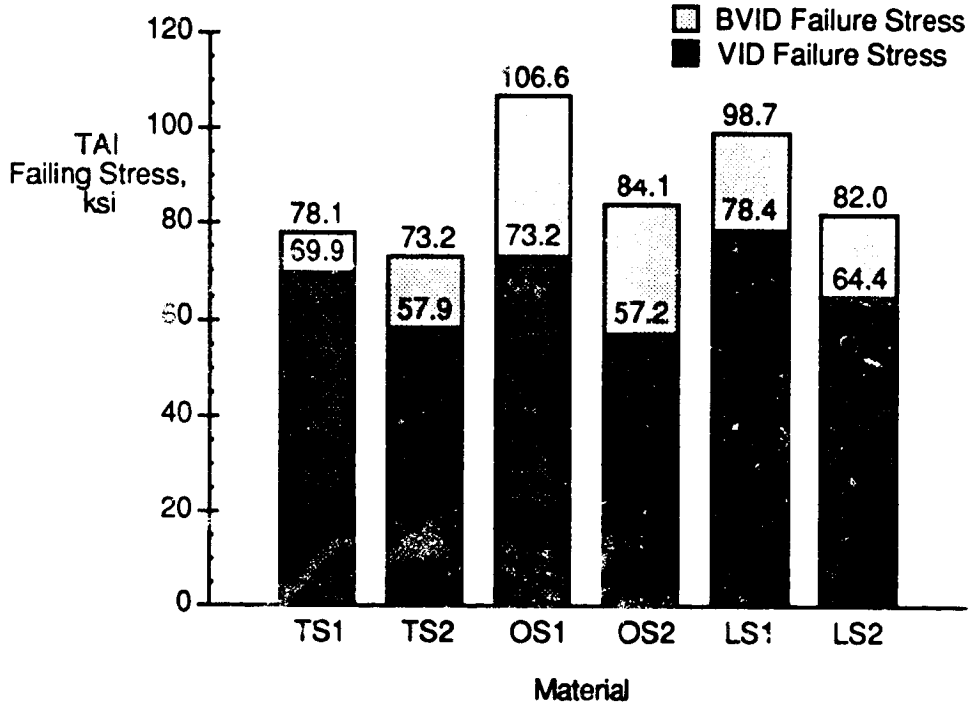

Figure 33. Tension Strength of 3-D Weaves with BVID (15.39 ft•lbs) and VID (62.86 ft•lbs).

The 3-D Weaves tended to exhibit their best performance in tension. Although the extent of damage from impact was generally higher than that of many of the other material architectures, the failing stresses obtained from these materials were typically higher. Failing stresses for the OS1 specimens averaged 106.6 ksi, better that any other material form examined in this study. Only the 32 ply Stitched Uniweave came within 10% of this value. The best performing 2-D Braid offered 30% less load carrying capability at the Barely Visible Impact Damage impact level.

Residual Strength, expressed as a percentage of unnotched strength, is shown in Figure 34 for each of the six 3-D Weaves. Data from both the lower Barely Visible Impact Damage level and the upper Visible Impact Damage level are shown in each figure.

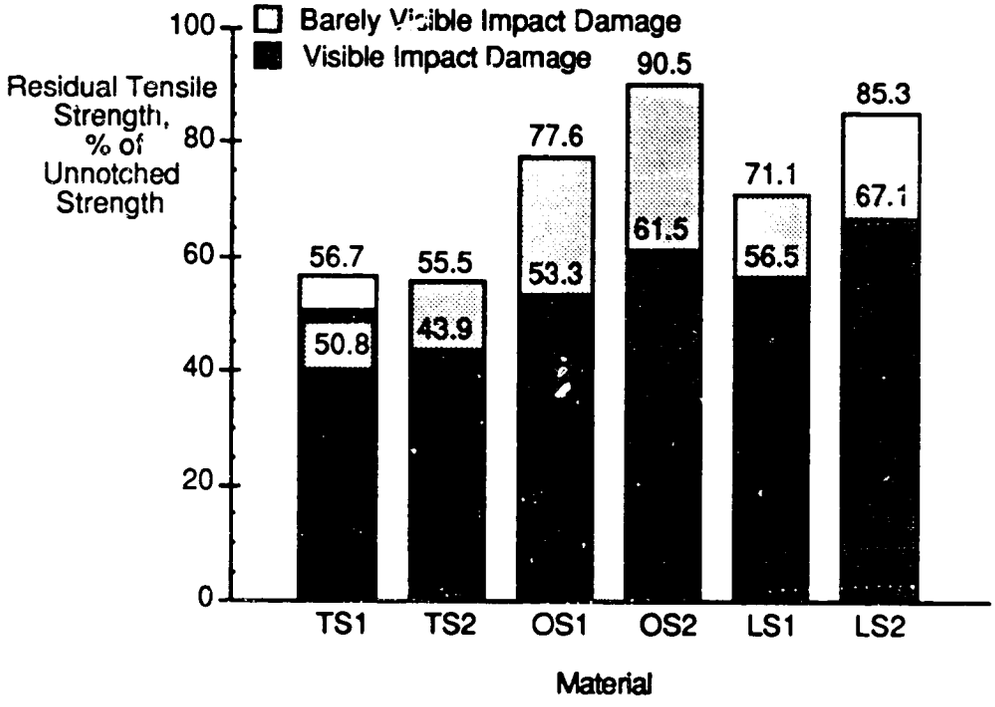

Figure 34. Damage Tolerance of 3-D Weaves with BVID (15.39 ft•lbs) and VID (62.86 ft•lbs).

The data indicate that the OS2 material retained better than 90% of its unnotched strength, again outperforming any other architecture evaluated in tension.

A comparison of the effect of fiber bundle size in tension produces somewhat different observations than those obtained in compression. The failing stress was always greater for the materials with the larger fiber bundles but the percentage strength retention trends were generally reversed. Residual strength was not only about equal for the TS1 and TS2 materials, it was also significant lower than the other architectures.

Figures 35 and 36 allow a comparison of the best and worst response to damage tolerance for all the material architectures in both tension and compression. Figure 35 shows the results of the compression testing while Figure 36 illustrates the tension data. Both figures display results obtained for the Visible Impact Damage and Barely Visible Impact Damage impact levels.

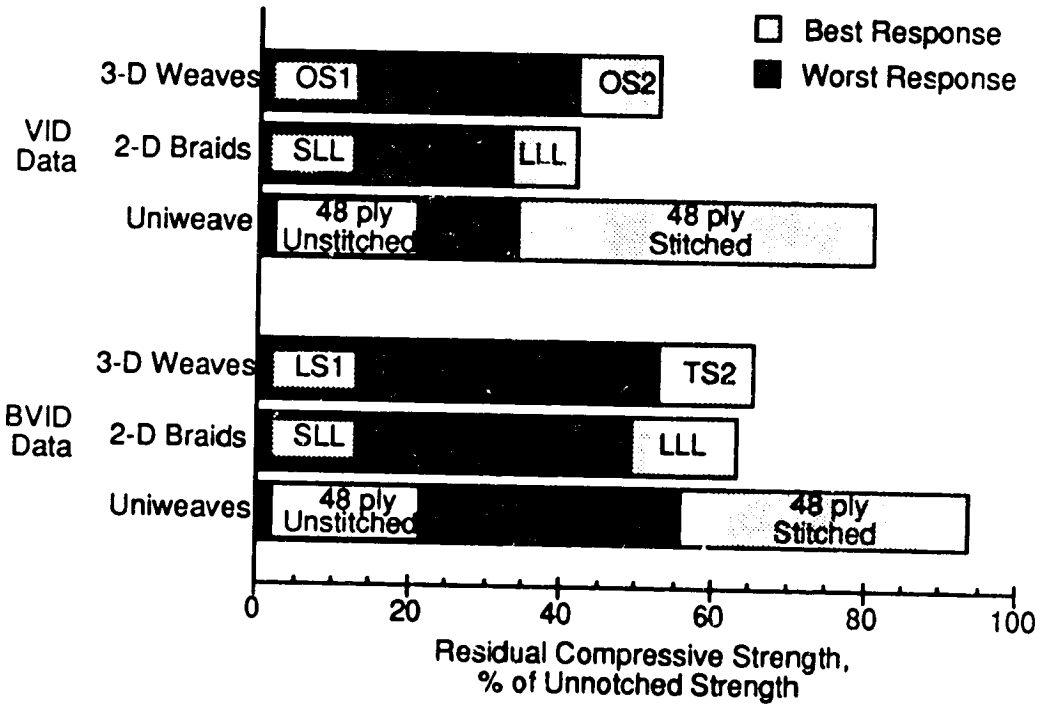

Figure 35. Summary of the Compression After Impact Response of 3-D Weaves, 2-D Braids, and Uniweaves with BVID (15.39 ft•lbs) and VID (62.86 ft•lbs) Impacts.

An examination of Figure 35 shows that stitching excels at reducing the effect of damage at both the Visible Impact Damage and Barely Visible Impact Damage impact levels. The 2-D braids and 3-D weaves show little improvement in damage tolerance over unstitched uniweaves. Recall that damage resistance was also rather poor with these materials.

An examination of Figure 36 shows that stitching, which excels at reducing damage growth in compression, does not appear to enhance damage tolerance as significantly in tension. Overall, the 2-D braids offer little tolerance to impact damage in compression but have moderately good response in tension. The 3-D weaves, which offered reasonably good damage tolerance in compression, outperform all the other textile architectures in tension. This result is surprising, given the poor damage resistance of the 3-D weaves.

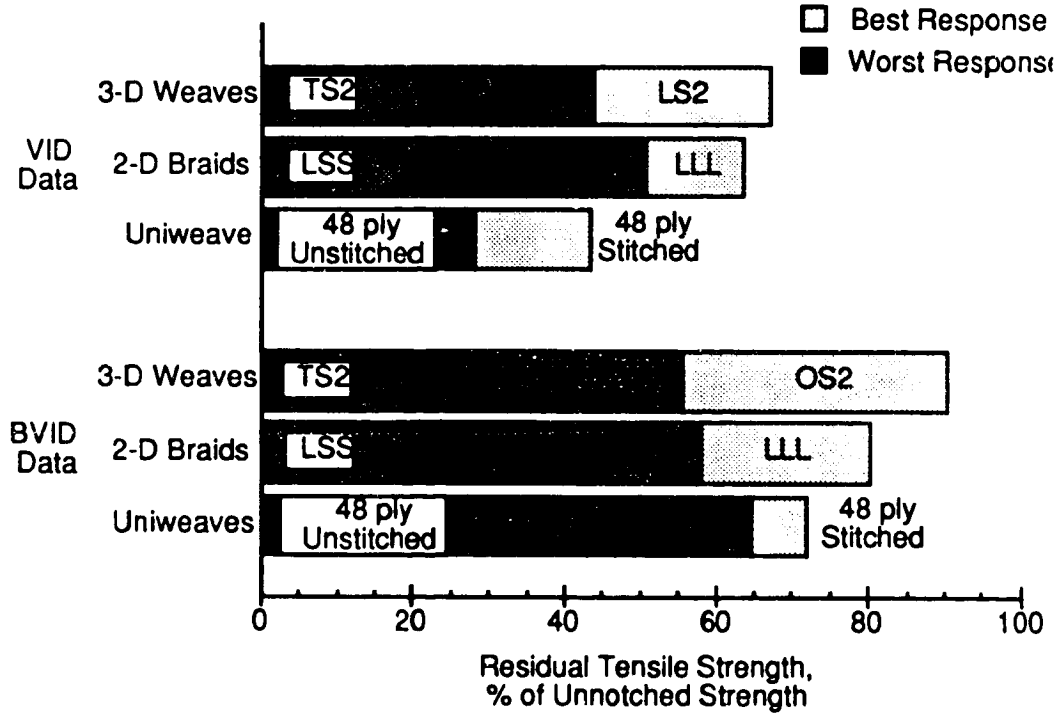

Figure 36. Summary of the Tension After Impact Response of 3-D Weaves, 2-D Braids, and Uniweaves with BVID (15.39 ft•lbs) and VID (62.86 ft•lbs) Impacts.

Findings and Conclusions

An evaluation of impact damage resistance and impact damage tolerance of stitched and unstitched uniweaves, 2-D braids, and 3-D weaves was conducted. Four different thicknesses of the uniweave material were tested. Only one thickness was evaluated with the braids and weaves but several variations of the braiding and weaving parameters were tested. All of the materials were subjected to either quasi-static indentation or low velocity (large mass) impacts and then loaded in tension or compression to measure residual strength.

Damage Resistance

Stitching of the uniweaves resulted in significant improvements in damage resistance. The stitched materials had significantly less damage area and higher peak impact forces than the unstitched materials. Damage resistance was better at the higher impact energies (VID levels) but the largest improvement was seen at the Mean Impact Damage level (Fig. 11).

The LLS, LSS, and SLL 2-D braided materials all behaved in a similar fashion at both impact energy levels. The LLL $[0_{75K}/\pm70_{15K}]46\%$ architecture showed the least resistance to impact with 50% more damage area than the best performing LSS $[0_{6K}/\pm45_{15K}]12\%$ at the severe impact damage level. With the braids, the difference in damage area between the BVID level and the VID level was smaller than that obtained with the uniweaves.

All the 3-D woven materials demonstrated comparable damage resistance at the low impact energy level. The weaves had less damage area on average at the low BVID level than the braids but more than the uniweaves. Damage resistance was similar to the braids at the VID impact level. The OS1 material had the worst resistance of the 3-D weaves with 53% more damage area than the best performing TS1 at the severe impact damage level.

Damage Tolerance

Stitching improved the compression after impact (CAI) strength at all impact energy levels. Stitched 48 ply CAI specimens retained 94% of their unnotched strength. Stitching improved strength in tension (TAI) at the mean and VID impact levels but not significantly at the lower BVID impact level. Stitched 48 ply TAI specimens retained 72% of their unnotched strength. In all CAI and TAI experiments, strength was always above 40 ksi. Stitching improved the uniweaves' damage tolerance at all impact energy levels. It was also noted that damage tolerance tended to increase with increasing plate thickness.

The residual strength of the 2-D braids was better in tension than in compression. At the BVID impact damage energy level, the LLL $[0_{75K}/\pm 70_{15K}]46\%$ retained 80% of its unnotched strength in tension, but only 63% of its unnotched strength in compression. The LLS $[0_{36K}/\pm 45_{15K}]46\%$ material had the least damage area but there was no significant improvement in strength retention over the other braids.

The 3-D weaves also had better damage tolerance in tension than in compression. At the BVID impact level, the OS2 retained 90% of its unnotched strength in tension but only 65% in compression. None of the weaves had outstanding performance in compression. In tension the TS2 and OS2 materials were noticeably better that any of the other weaves. The OS2 specimen retained 90% of its unnotched strength. Only the 48 ply stitched uniweave came within 10% of this performance.

Tow Size Effects

The effect of fiber bundle size was compared wherever possible. Two of the 2-D braids were constructed with the same percentage of axial yarns and the same braid angle but using braided tows 2.5 times different in size. The 3-D weaves were constructed in pairs with the "1" materials having yarn bundles twice as large as the "2" materials.

The damage resistance of the 2-D braids and 3-D weaves were influenced by tow size in a dissimilar fashion. The 2-D braids with the larger fiber bundle sizes tended to have greater damage area, regardless of the impact energy level. The 3-D weaves with the larger tow sizes typically had less damage area.

It was found that tow size may affect the damage tolerance of the 2-D braids and 3-D weaves. With the 2-D braids, the larger tow size resulted in a decrease in post-impact strength but an improvement in the percentage of strength retained after impact (expressed as a percentage of the materials' un-impacted compression strength). The 3-D weaves' response was opposite than of the 2-D braids. In this case the large fiber bundles resulted in an increase in post-impact strength but a reduction in the percentage of strength retention.

The behavior of the 2-D braids with varying tow size was always consistent. Regardless of the impact energy or whether the specimen was tested in compression or tension, the post-impact strengths always decreased and the percentage strength retention always increased in the specimens with the larger fiber bundles. The behavior of the 3-D weaves was also very consistent in both tension and compression, although some aberrations to these trends were noticed. Specifically, the OS2 material had higher strength in compression and the TS2 had lower percentage strength retention. These responses were the opposite of the other weaves. The cause of this response is unclear but may be architecturally dependent.

References

1. Falcone, A., Dursch, H., Nelson, K., Avery, W., "Resin Transfer Molding of Textile Composites," NASA CR. 191505, March 1993.

2. "NASA/Aircraft Industry Standard Specification for Graphite Fiber/Toughened Thermoset Resin Composite Material", NASA Reference Publication 1142, June 1985

Appendix A: Data Tables

Table A1. Stitched and Unstitched Uniweaves Impact to Produce Barely Visible Impact Damage.

		Damage Area, in^2	Peak Impact Force, lbf	CAI, ksi	TAI, ksi
48 ply	Stitched	1.1109	3424.8	46.156	75.580
	Unstitched	2.7249	3013.9	29.136	79.203
32 ply	Stitched	0.53000	1686.2	45.170	79.166
	Unstitched	1.1714	1564.1	37.056	95.210
24 ply	Stitched	0.43660	1189.5	40.818	78.933
	Unstitched	0.83420	1172.5	32.699	91.526
16 ply	Stitched	0.26770	639.70	33.461	78.857
	Unstitched	0.36980	636.13	38.119	89.489

Table A2. Stitched and Unstitched Uniweaves Impact to Produce Mean Impact Damage.

		Damage Area, in^2	Peak Impact Force, lbf	CAI, ksi	TAI, ksi
48 ply	Stitched	1.9641	4375.7	-	51.163
	Unstitched	5.6625	4038.4	-	45.547
32 ply	Stitched	1.2505	2297.5	-	53.427
	Unstitched	2.6642	2075.8	-	47.908
24 ply	Stitched	0.8650	1559.7	-	54.994
	Unstitched	1.040	1361.8	-	42.667
16 ply	Stitched	0.4750	824.1	-	51.228
	Unstitched	0.7719	686.5	-	46.237

Table A3. Stitched and Unstitched Uniweaves Impact to Produce Visible Impact Damage.

		Damage Area, in^2	Peak Impact Force, lbf	CAI, ksi	TAI, ksi
48 ply	Stitched	4.4634	4732.1	39.941	45.790
	Unstitched	5.8962	3678.7	17.858	34.472
32 ply	Stitched	1.8753	2725.0	40.699	45.052
	Unstitched	3.6781	2228.2	20.476	37.426
24 ply	Stitched	1.1848	1817.5	37.413	46.705
	Unstitched	2.7856	1384.6	24.8	38.391
16 ply	Stitched	0.6245	992.86	33.436	44.476
	Unstitched	2.4947	699.61	28.436	35.148

Table A4. 2-D Braids Impact at 15.39 ft•lbs to Produce Barely Visible Impact Damage.

	Damage Area, in^2	Peak Impact Force, lbf	CAI, ksi	TAI, ksi
SLL	3.3549	2465.6	34.662	75.280
LLS	3.1097	2311.4	32.166	71.424
LLL	3.8746	2279.6	30.824	69.936
LSS	2.5330	2525.5	25.629	30.784

Table A5. 2-D Braids Impact at 62.86 ft•lbs to Produce Visible Impact Damage.

	Damage Area, in^2	Peak Impact Force, lbf	CAI, ksi	TAI, ksi
SLL	3.2773	2503.4	23.260	54.704
LLS	3.4627	2483.6	24.040	50.300
LLL	4.4300	2596.3	20.285	55.520
LSS	2.9600	2722.3	17.625	26.940

Table A6. 3-D Weaves Impact at 15.39 ft•lbs to Produce Barely Visible Impact Damage.

	Damage Area, in^2	Peak Impact Force, lbf	CAI, ksi	TAI, ksi
TS1	2.1347	2495.8	45.255	78.0640
TS2	2.4361	2561.5	41.543	73.2160
LS1	2.7438	2343.9	46.992	106.592
LS2	2.3496	2379.0	45.955	84.0800
OS1	2.6823	2482.7	40.504	98.7440
OS2	-	2693.0	36.336	82.0000

Table A7. 3-D Weaves Impact at 62.86 ft•lbs to Produce Visible Impact Damage.

	Damage Area, in^2	Peak Impact Force, lbf	CAI, ksi	TAI, ksi
TS1	2.9930	2778.0	39.327	69.8720
TS2	3.8140	2753.7	31.296	57.9200
LS1	4.6270	2824.2	34.944	73.2000
LS2	3.6463	2540.2	40.615	57.1520
OS1	5.4120	3135.0	32.383	78.4350
OS2	-	3391.0	28.408	64.4480

REPORT DOCUMENTATION PAGE

Form Approved
OMB No. 0704-0188

1. AGENCY USE ONLY (*Leave blank*)	2. REPORT DATE	3. REPORT TYPE AND DATES COVERED
	December 1995	Contractor Report

4. TITLE AND SUBTITLE

Evaluation of the Impact Response of Textile Composites

5. FUNDING NUMBERS

Contract NAS1-19000

WU 505-63-50-04

6. AUTHOR(S)

M. A. Portanova

7. PERFORMING ORGANIZATION NAME(S) AND ADDRESS(ES)

Lockheed Martin Engineering & Sciences
144 Research Drive
Hampton, VA 23666

8. PERFORMING ORGANIZATION REPORT NUMBER

9. SPONSORING/MONITORING AGENCY NAME(S) AND ADDRESS(ES)

National Aeronautics and Space Administration
Langley Research Center
Hampton, VA 23681-0001

10. SPONSORING/MONITORING AGENCY REPORT NUMBER

NASA CR-198265

11. SUPPLEMENTARY NOTES

Langley Technical Monitor: I. S. Raju

12a. DISTRIBUTION/AVAILABILITY STATEMENT

Unclassified - Unlimited
Subject Category 24

12b. DISTRIBUTION CODE

13. ABSTRACT (*Maximum 200 words*)

An evaluation of the impact damage resistance and impact damage tolerance of stitched and unstitched uniweaves, 2-D braids, and 3-D weaves was conducted. Uniweave laminates were tested at four thicknesses to determine the sensitivity of the tests to this parameter. Several braid and weave parameters were also varied to establish their effect on damage resistance and tolerance. All of the materials were subjected to either quasi-static indentation or low velocity (large mass) impacts and then loaded in tension or compression to measure residual strength.

Experimental results indicate that stitching significant improves the uniweaves' damage resistance. The 2-D braids and 3-D weaves offered less damage resistance than the stitched materials. Stitching also improved the compression after impact (CAI) and tension after impact (TAI) strengths of the uniweave materials.

14. SUBJECT TERMS

Low Velocity Impact, Static Indentation, Damage Tolerance, Damage Resistance, Textile Composites, Specimen Geometry, Size Effects,s

15. NUMBER OF PAGES

53

16. PRICE CODE

A04

17. SECURITY CLASSIFICATION OF REPORT	18. SECURITY CLASSIFICATION OF THIS PAGE	19. SECURITY CLASSIFICATION OF ABSTRACT	20. LIMITATION OF ABSTRACT
Unclassified	Unclassified		

NSN 7540-01-280-5500

Standard Form 298 (Rev. 2-89)
Prescribed by ANSI Std. Z39-18
298-102

END

DATE

FILMED

FEB 13 1996

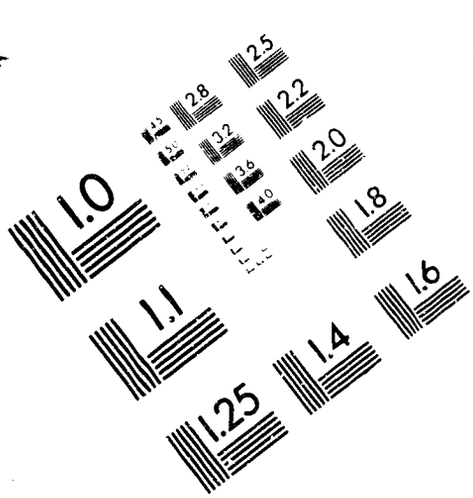

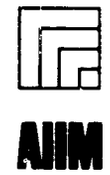

Association for Information and Image Management
1100 Wayne Avenue, Suite 1100
Silver Spring, Maryland 20910
301/587-8202

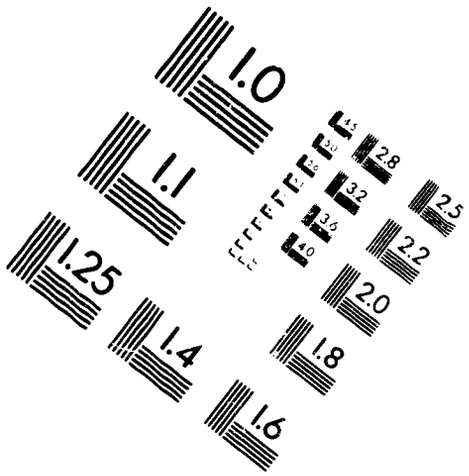

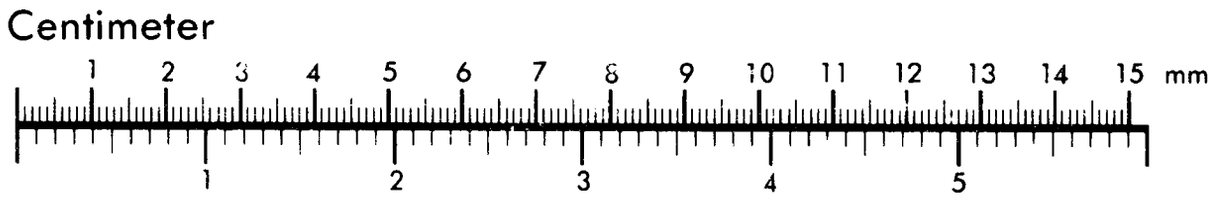

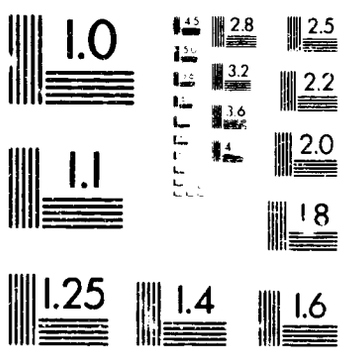

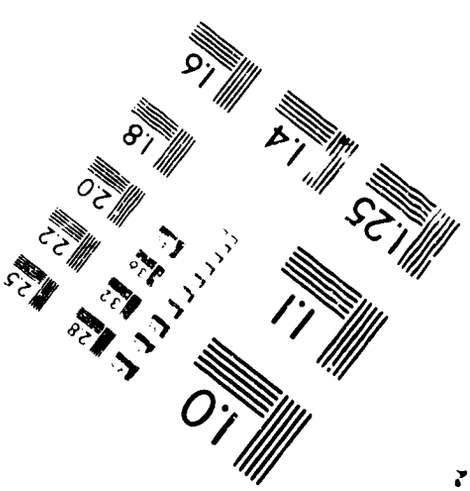

MANUFACTURED TO AIIM STANDARDS
BY APPLIED IMAGE, INC.